

Comparison of Simulated to Measured Groundwater Nitrate-N Concentrations from SBR Discharges in the Taupo Catchment

Prepared by:
Greg Barkle (Aqualinc Research Ltd) and
Fuli Wang (Lincoln Environmental)

For:
Environment Waikato
PO Box 4010
HAMILTON EAST

ISSN: 1172-4005

June 2005

Document #: 1043954

Peer reviewed by:
John Hadfield

Signature



Date

June 2006

Approved for release
by:
Dr Vivienne Smith

Signature



Date

June 2006



Comparison of Simulated to Measured Groundwater Nitrate-N Concentrations from SBR Discharges in the Taupo Catchment

Prepared for Environment Waikato

Report No H05012/1

June 2005



Disclaimer:

This report has been prepared solely for the benefit of Environment Waikato. No liability is accepted by Aqualinc Research Ltd or any employee or sub-consultant of this Company with respect to its use by any other person.

This disclaimer shall apply notwithstanding that the report may be made available to other persons for an application for permission or approval or to fulfil a legal requirement.

| Quality Control | | | |
|------------------------|--|------------------------|-------------|
| Client: | Environment Waikato | | |
| Report reference: | Title: Comparison of Simulated to Measured Groundwater Nitrate-N Concentrations from SBR Discharges in the Taupo Catchment | No: H05012/1 | |
| Prepared by: | Greg Barkle (Aqualinc Research Ltd) and Fuli Wang (Lincoln Environmental) | | |
| Reviewed by: | Fuli Wang | Approved for issue by: | Greg Barkle |
| Date issued: | June 2005 | Project No: | H05012 |

| Document History | | | |
|-------------------------|--|----------------------|--------------------|
| Version: 1 | Status: Draft, for Client's review | Author: G Barkle | Reviewer: F Wang |
| Date: 16/6/05 | Doc ID: H05012_EW SBR GW modelling (Taupo)_rpt1_draft.doc | Typist: L Sallabanks | Approver: G Barkle |
| Version: 2 | Status: 2 nd draft, for Client's review | Author: G Barkle | Reviewer: F Wang |
| Date: 22/8/05 | Doc ID: H05012_EW SBR GW modelling (Taupo)_rpt1_draft2.doc | Typist: R Grant | Approver: G Barkle |
| Version: 3 | Status: Final | Author: G Barkle | Reviewer: F Wang |
| Date: 22/9/05 | Doc ID: H05012_EW SBR GW modelling (Taupo)_rpt1_final.doc | Typist: R Grant | Approver: G Barkle |

© All rights reserved. This publication may not be reproduced or copied in any form, without the permission of the Client. Such permission is to be given only in accordance with the terms of the Client's contract with Aqualinc Research Ltd. This copyright extends to all forms of copying and any storage of material in any kind of information retrieval system.

TABLE OF CONTENTS

| | Page |
|---|-----------|
| Executive Summary | 1 |
| 1 Introduction | 2 |
| 2 FEMWATER-N Mathematical Descriptions..... | 3 |
| 3 Monitoring Data and Site Layout of Acacia Bay SBR Discharge..... | 4 |
| 4 Acacia Bay SBR Model Setup and Input Data | 4 |
| 5 Analyses of Measured Nitrate-N Concentrations at Acacia Bay SBR Monitoring Wells | 6 |
| 6 Acacia Bay SBR Model Calibration | 10 |
| 7 Acacia Bay SBR Model Sensitivity Analysis..... | 11 |
| 7.1 Hydraulic Conductivity | 11 |
| 7.2 Rate of Denitrification | 12 |
| 7.3 Rate of Nitrification | 14 |
| 7.4 Dispersion Coefficient | 17 |
| 7.5 Spatial Variation in Hydraulic Conductivity | 20 |
| 8 Monitoring Data and Site Layout of Kinloch SBR Discharge | 21 |
| 9 Kinloch SBR Model Setup and Input Data..... | 22 |
| 10 Analyses of Measured Nitrate-N Concentrations at Kinloch SBR Monitoring Wells | 24 |
| 11 Kinloch SBR Model Calibration | 26 |
| 12 Kinloch SBR Model Sensitivity Analysis..... | 31 |
| 12.1 Hydraulic Conductivity | 31 |
| 12.2 Rate of Denitrification | 31 |
| 12.3 Rate of Nitrification | 35 |
| 12.4 Dispersion Coefficient | 39 |
| 13 Summary | 45 |
| 14 References | 46 |

List of Tables:

| | |
|---|----|
| Table 1: Calibrated parameters for Acacia Bay SBR model and range over which they were investigated | 10 |
| Table 2: Acacia Bay slug test data (Hadfield and Piper, 2005)..... | 11 |
| Table 3: Estimation of pore water velocity based on nitrate-N peaks in monitoring wells .. | 25 |
| Table 4: Kinloch slug test data (Hadfield and Piper, 2005) | 25 |
| Table 5: Calibrated parameters for Kinloch SBR model and range over which they were investigated | 26 |

List of Figures:

| | |
|---|----|
| Figure 1: Plan view of the numerical mesh, locations of effluent discharge trenches (two rectangles in the dense grid area), and monitoring wells (dots) for the Acacia Bay SBR model. | 4 |
| Figure 2: Measured nitrate-N concentration of the discharged effluent from the Acacia Bay SBR | 6 |
| Figure 3: Comparison between measured and simulated BTCs at the control monitoring well | 7 |
| Figure 4: Comparison between measured and simulated BTCs at monitoring well 1 | 7 |
| Figure 5: Comparison between measured and simulated BTCs at monitoring well 2 | 8 |
| Figure 6: Comparison between measured and simulated BTCs at monitoring well 3 | 8 |
| Figure 7: Comparison between measured and simulated BTCs at monitoring well 4 | 9 |
| Figure 8: Simulated BTC at the control well as affected by the rate of denitrification (V_{den}). Results for $V_{den}=0.2$ and 0.1 are plotted under the $V_{den}=0.01$ line. | 12 |
| Figure 9: Simulated BTC at monitoring well 1 as affected by the rate of denitrification (V_{den}) | 12 |
| Figure 10: Simulated BTC at monitoring well 2 as affected by the rate of denitrification (V_{den}) | 13 |
| Figure 11: Simulated BTC at monitoring well 3 as affected by the rate of denitrification (V_{den}) | 13 |
| Figure 12: Simulated BTC at monitoring well 4 as affected by the rate of denitrification (V_{den}) | 14 |
| Figure 13: Simulated BTC at the control well as affected by the rate of nitrification (V_{nit}). Results for $V_{nit}=0.005$ and 0.01 plotted under the $V_{nit}=0.1$ per day. | 15 |

| | | |
|---------------|--|----|
| Figure 14: | Simulated BTC at monitoring well 1 as affected by the rate of nitrification (V_{nit})..... | 15 |
| Figure 15: | Simulated BTC at monitoring well 2 as affected by the rate of nitrification (V_{nit})..... | 16 |
| Figure 16: | Simulated BTC at monitoring well 3 as affected by the rate of nitrification (V_{nit})..... | 16 |
| Figure 17: | Simulated BTC at monitoring well 4 as affected by the rate of nitrification (V_{nit})..... | 17 |
| Figure 18: | Simulated BTC at the control well as affected by longitudinal dispersivity (AL)..... | 18 |
| Figure 19: | Simulated BTC at monitoring well 1 as affected by longitudinal dispersivity (AL)..... | 18 |
| Figure 20: | Simulated BTC at monitoring well 2 as affected by longitudinal dispersivity (AL)..... | 19 |
| Figure 21: | Simulated BTC at monitoring well 3 as affected by longitudinal dispersivity (AL)..... | 19 |
| Figure 22: | Simulated BTC at monitoring well 4 as affected by longitudinal dispersivity (AL)..... | 20 |
| Figure 23: | Monte Carlo simulated BTCs (lines) compared with measured BTCs at monitoring wells (dots)..... | 21 |
| Figure 24(a): | Plan view of the numerical mesh, locations of effluent discharge trench (rectangle in red colour) and monitoring wells (dots) for the Kinloch SBR model..... | 23 |
| Figure 24(b): | Locations of sampling wells at the Kinloch site (sampling well 1 not shown). Rectangle represents discharge trench and circles represent wells. | 23 |
| Figure 25: | Nitrate-N concentration of discharged effluent vs simulation time | 24 |
| Figure 26: | Comparison between measured and simulated BTCs at monitoring well 1 (control) | 26 |
| Figure 27: | Comparison between measured and simulated BTCs at monitoring well 5..... | 27 |
| Figure 28: | Comparison between measured and simulated BTCs at monitoring well 6..... | 27 |
| Figure 29: | Comparison between measured and simulated BTCs at monitoring well 7 for various values of hydraulic conductivity | 28 |
| Figure 30: | Comparison between measured and simulated BTCs at monitoring well 2 for various values of hydraulic conductivity | 28 |
| Figure 31: | Comparison between measured and simulated BTC's at monitoring well 3 for various values of hydraulic conductivity | 29 |
| Figure 32: | Comparison between measured and simulated BTCs at monitoring well 4 for various values of hydraulic conductivity | 29 |

| | | |
|------------|--|----|
| Figure 33: | Comparison between measured and simulated BTCs at monitoring well 8 for various values of hydraulic conductivity | 30 |
| Figure 34: | Comparison between measured and simulated BTCs at monitoring well 9 for various values of hydraulic conductivity | 30 |
| Figure 35: | Simulated BTC at monitoring well 6 as affected by the rate of denitrification (Vden) | 32 |
| Figure 36: | Simulated BTC at monitoring well 7 as affected by the rate of denitrification (Vden) | 32 |
| Figure 37: | Simulated BTC at monitoring well 2 as affected by the rate of denitrification (Vden) | 33 |
| Figure 38: | Simulated BTC at monitoring well 3 as affected by the rate of denitrification (Vden) | 33 |
| Figure 39: | Simulated BTC at monitoring well 4 as affected by the rate of denitrification (Vden) | 34 |
| Figure 40: | Simulated BTC at monitoring well 8 as affected by the rate of denitrification (Vden) | 34 |
| Figure 41: | Simulated BTC at monitoring well 9 as affected by the rate of denitrification (Vden) | 35 |
| Figure 42: | Simulated BTC at monitoring well 6 as affected by the rate of nitrification (Vnit)..... | 36 |
| Figure 43: | Simulated BTC at monitoring well 7 as affected by the rate of nitrification (Vnit)..... | 36 |
| Figure 44: | Simulated BTC at monitoring well 2 as affected by the rate of nitrification (Vnit)..... | 37 |
| Figure 45: | Simulated BTC at monitoring well 3 as affected by the rate of nitrification (Vnit)..... | 37 |
| Figure 46: | Simulated BTC at monitoring well 4 as affected by the rate of nitrification (Vnit)..... | 38 |
| Figure 47: | Simulated BTC at monitoring well 8 as affected by the rate of nitrification (Vnit)..... | 38 |
| Figure 48: | Simulated BTC at monitoring well 9 as affected by the rate of nitrification (Vnit)..... | 39 |
| Figure 49: | Simulated BTC at monitoring well 1 (control) as affected by longitudinal dispersivity (AL)..... | 40 |
| Figure 50: | Simulated BTC at monitoring well 5 as affected by longitudinal dispersivity (AL)..... | 40 |
| Figure 51: | Simulated BTC at monitoring well 6 as affected by longitudinal dispersivity (AL)..... | 41 |

| | Page |
|--|------|
| Figure 52: Simulated BTC at monitoring well 7 as affected by longitudinal dispersivity (AL)..... | 41 |
| Figure 53: Simulated BTC at monitoring well 2 as affected by longitudinal dispersivity (AL)..... | 42 |
| Figure 54: Simulated BTC at monitoring well 3 as affected by longitudinal dispersivity (AL)..... | 43 |
| Figure 55: Simulated BTC at monitoring well 4 as affected by longitudinal dispersivity (AL)..... | 43 |
| Figure 56: Simulated BTC at monitoring well 8 as affected by longitudinal dispersivity (AL)..... | 44 |
| Figure 57: Simulated BTC at monitoring well 9 as affected by longitudinal dispersivity (AL)..... | 44 |

EXECUTIVE SUMMARY

The propagation of a groundwater nitrate plume resulting from the discharge of treated effluent from sequential batch reactors at Acacia Bay site and Kinloch are modelled using a three-dimensional flow and contaminant transport numerical model (FEMWATER-N). The models simulate the transport and transformation of ammonium-N, nitrate-N and dissolved organic carbon in the vadose zone and aquifer. Nitrification and denitrification are described by first-order and multiple Monod kinetics models, respectively.

The models have been calibrated by comparing simulated nitrate-N results with measured concentrations at five monitoring wells for the Acacia Bay site and nine wells for the Kinloch site. The models were able to adequately describe the nitrate concentrations in most monitoring wells. However, the verification of the dynamics of the groundwater nitrate-N was hampered by the time between samplings in the monitoring wells.

Sensitivity analyses showed that nitrate-N concentrations at sampling wells were sensitive to model parameters in the order of hydraulic conductivity, rate of denitrification, rate of nitrification, and dispersivity.

Preliminary Monte Carlo numerical simulations at the Acacia Bay site demonstrated that the heterogeneity of aquifer hydraulic conductivity may be the major factor contributing to the discrepancy between simulated and measured concentrations at the sampling wells.

1 INTRODUCTION

A previous study (Barkle and Wang, 2003) simulation models were developed of the groundwater systems around the Taupo District Council's (TDC) wastewater treatment plants at Acacia Bay and Kinloch. The models were designed to investigate the effects of the discharge of treated domestic effluent from the sequential batch reactors (SBR) into shallow trenches and subsequently into the shallow groundwater. A preliminary test of the models against measured groundwater monitoring data (Barkle, 2004) identified improvements required in the model input data and the parameter sets used for both simulation models. The recommendations for improvement included:

- The model domain should be decreased so that a greater resolution of the predicted nitrate-N concentrations around the monitored area can be obtained.
- The dissimilitatory nitrate-N reduction and/or denitrification rates at the Acacia Bay SBR discharge site should be investigated and this information used to improve the representation of these processes in the FEMWATER-N model.
- The hydraulic properties of the aquifers at both sites should be determined from tracer and/or pump tests.
- Upstream nitrate-N concentrations in the model should be based on monitoring data from the control wells.
- Improvements in the representations of the layout of the SBR discharge trenches are required.
- The effluent input files should be based on actual weekly samplings not long termed averaged data.
- The simulated nitrate-N concentrations should be determined for the average nitrate-N concentration over the screened depth of each of the monitoring wells.
- Hydraulic gradients should be based on measured data.

Based on these suggested improvements, new FEMWATER-N models were set up to simulate the transport and transformation of nitrogen and carbon at the Acacia Bay and Kinloch SBR discharge sites. The simulated chemicals are ammonium-N, nitrate-N and dissolved organic carbon. Nitrification is simulated using a first-order kinetics model and denitrification is simulated as double Monod model (Wang *et al.*, 2003). New simulation results are compared to the monitoring data in this report. In addition, sensitivity analyses of the model parameters, which were not measured, on the simulated nitrate-N concentrations are also presented.

2 FEMWATER-N MATHEMATICAL DESCRIPTIONS

Measured data show that SBR treated effluent contains organic-N, ammonium and nitrate, and dissolved organic carbon (DOC). Assuming that the mineralisation of organic-N is fast when compared to other processes, we only simulate the transport of ammonium, nitrate and DOC, which may be described by the following partial differential equations:

$$\begin{aligned} \frac{\partial(\theta_l c_l^{AN})}{\partial t} + \frac{\partial(\rho_s c_s^{AN})}{\partial t} &= L(c_l^{AN}) - \mathfrak{R}_{nit}^N, \\ \frac{\partial(\theta_l c_l^S)}{\partial t} &= L(c_l^S) - \left(\frac{1}{y_{den}}\right) \mathfrak{R}_{den}^N \quad \text{and} \\ \frac{\partial(\theta_l c_l^{NN})}{\partial t} &= L(c_l^{NN}) + \mathfrak{R}_{nit}^N - \mathfrak{R}_{den}^N \end{aligned}$$

where c_l^{AN} , c_l^S and c_l^{NN} are concentrations of ammonium-N, substrate (DOC) and nitrate-N in the liquid phase (M/L³ water), respectively, c_s^{AN} is ammonium-N concentration in the solid phase (M/M solids) and is related to c_l^{AN} by the linear instantaneous adsorption equation, $c_s^{AN} = k_d c_l^{AN}$, θ_l is the volumetric fraction of the liquid phase (L³ water/L³ medium), ρ_s is the bulk density (M solids/L³ medium), y_{den} is the consumption ratio of N to C in denitrification, L is a differential operator representing solute advection and dispersion terms, \mathfrak{R}_{nit}^N and \mathfrak{R}_{den}^N are rates of nitrification and denitrification (M/T/L³ medium), respectively, expressed as:

$$\begin{aligned} \mathfrak{R}_{nit}^N &= V_{nit} c_l^{AN} \quad \text{and} \\ \mathfrak{R}_{den}^N &= V_{den} \frac{c_l^S}{K^S + c_l^S} \frac{c_l^{NN}}{K^{NN} + c_l^{NN}} \end{aligned}$$

where V_{nit} is the rate constant of nitrification (1/T), V_{den} is the maximum rate of denitrification (M/T/L³medium), K^{NN} and K^S are half rate concentrations of ammonium-N and carbon (M/L³), respectively. The reader is referred to Wang *et al.* (2003) for a full description of the model.

3 MONITORING DATA AND SITE LAYOUT OF ACACIA BAY SBR DISCHARGE

The reader is referred to Barkle (2004) for a full description of the Acacia Bay SBR site, the trench locations, the monitoring wells and the monitoring data.

4 ACACIA BAY SBR MODEL SETUP AND INPUT DATA

The model domain – 250 m long, 100 m wide and between 43 m and 52 m high – was divided into 15 numerical layers. The thickness of numerical layers increases from about 1.5 m in the zone near the top boundary to about 5.5 m in the zone near the bottom boundary. Each layer is divided into 962 numerical elements, with a total of 517 numerical nodes. The two effluent discharge trenches are divided into 45 elements. The numerical mesh is dense in the neighbourhood of the trenches and becomes gradually coarser away from trenches (Figure 1). The bottom of the trenches was treated as a specified flux boundary with weekly measured effluent discharge data as inputs. A uniform rainfall recharge rate was applied to the top boundary, except the area covered by the trenches. The upstream and downstream boundary conditions are specified as constant heads. The upstream groundwater head is 46 m (about 6 m below top boundary), while the downstream boundary is set to 41 m (about 2 m below top boundary). The distance between the boundaries is 250 m, and thus the hydraulic gradient is 2%.

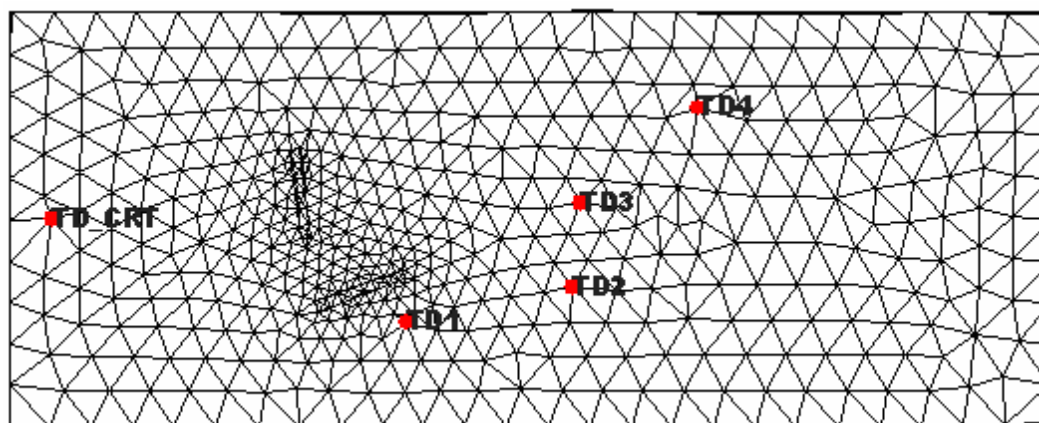


Figure 1: Plan view of the numerical mesh, locations of effluent discharge trenches (two rectangles in the dense grid area), and monitoring wells (dots) for the Acacia Bay SBR model.

The improvements in this model from that developed by previous work (Barkle and Wang, 2003) include:

- Correct orientation and layout of the SBR trenches;
- Upstream nitrate-N concentration based on measured data in the control well;
- Hydraulic gradient based on measured data (2%);
- Effluent input based on weekly samplings;
- Better resolution of the finite element grid; and
- Simulated nitrate-N concentration based on average concentration over the screened depth of the monitoring wells.

The model parameters that were not measured for this study include:

- Saturated hydraulic conductivity (later measured);
- Nitrification rate;
- Denitrification rate;
- Longitudinal dispersivity;
- Horizontal transverse dispersivity; and
- Vertical transverse dispersivity.

All parameters, except the vertical transverse dispersivity that was fixed at 10% of the horizontal transverse dispersivity, were calibrated by minimising the difference between the simulated nitrate-N concentrations and measured data (Section 4). A sensitivity analysis of the effect of these calibrated parameters on the simulated nitrate-N concentrations was completed.

The initial nitrate-N concentration in the model domain is 0.01 mg/l and nitrate-N concentration of groundwater coming in through the upstream boundary is 0.05 mg/l (based on observations at the control well). The rate of water drainage from top soils and the nitrate-N concentration of this drainage water were set at 1 mm/day (Hadfield, 1995) and 0.0 mg/l, respectively.

5 ANALYSES OF MEASURED NITRATE-N CONCENTRATIONS AT ACACIA BAY SBR MONITORING WELLS

As is shown in Figure 2, nitrate-N concentration in the discharged SBR effluent had a large peak on the 516th day (model simulation time) and a trend of increasing nitrate-N with time from day 1000. The large nitrate-N peak was observed at monitoring wells 1 and 2 (Figure 4 and Figure 5), but an accurate peak time, between 489 and 615 days, could not be estimated due to the long time (126 days) between samplings. The trend of nitrate-N concentration increasing with time was observed in monitoring well 1 after 700 days (using total N, Figure 4) and in well 2 after 1100 day (Figure 5). The reason that this trend was only evident in the total N in monitoring well 1 was due to the possibility of dissimilitatory nitrate-N reduction occurring close to the trench as discussed by Barkle (2004). This increasing trend of nitrate-N with time was not apparent in monitoring wells 3 and 4 (Figure 5 and Figure 6), which are further downstream of the discharge trenches.

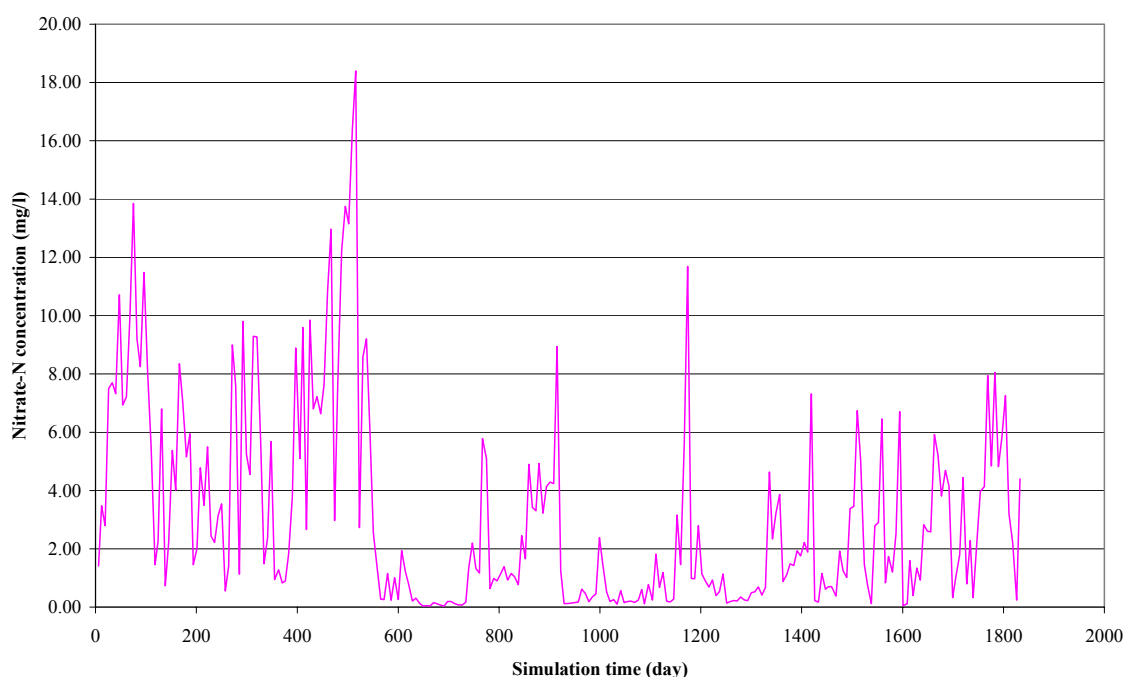


Figure 2: Measured nitrate-N concentration of the discharged effluent from the Acacia Bay SBR

Figure 3 shows that simulated nitrate-N concentrations at the control well are much higher than measured ones when a small hydraulic conductivity (1 m/day) was used. This is due to the influence of the SBR effluent discharge on nitrate-N concentration in the “control” well under the slow groundwater flow conditions. Since measurements showed that nitrate-N concentration at the control well was not actually affected by effluent discharge, aquifer hydraulic conductivity must be higher than 1 m/day.

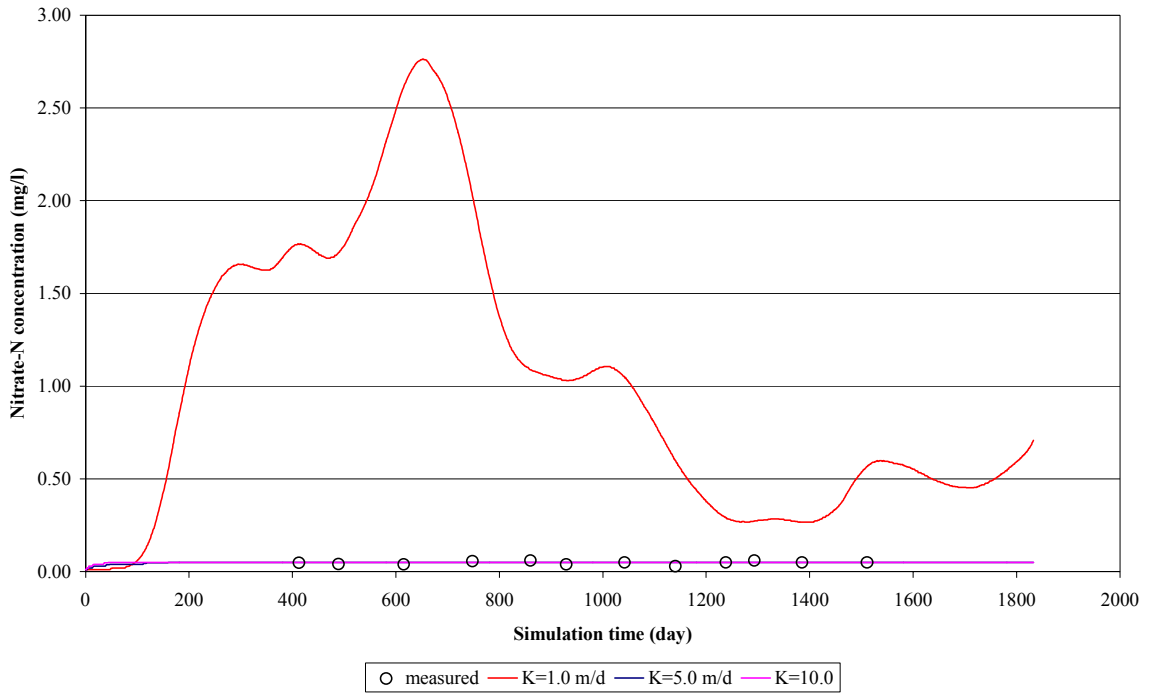


Figure 3: Comparison between measured and simulated BTCs at the control monitoring well

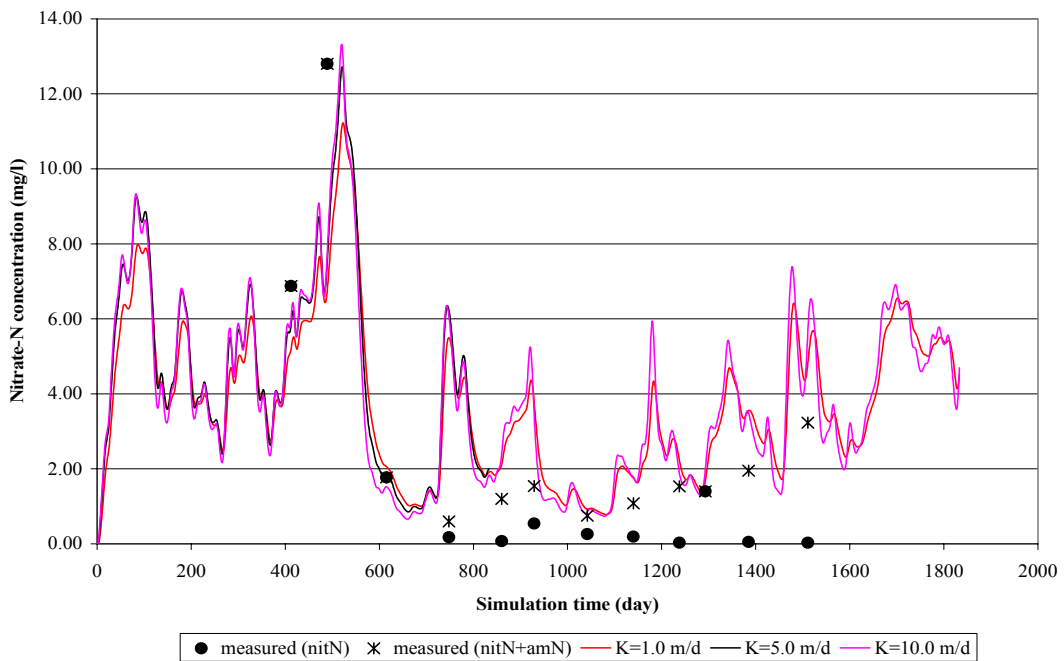


Figure 4: Comparison between measured and simulated BTCs at monitoring well 1

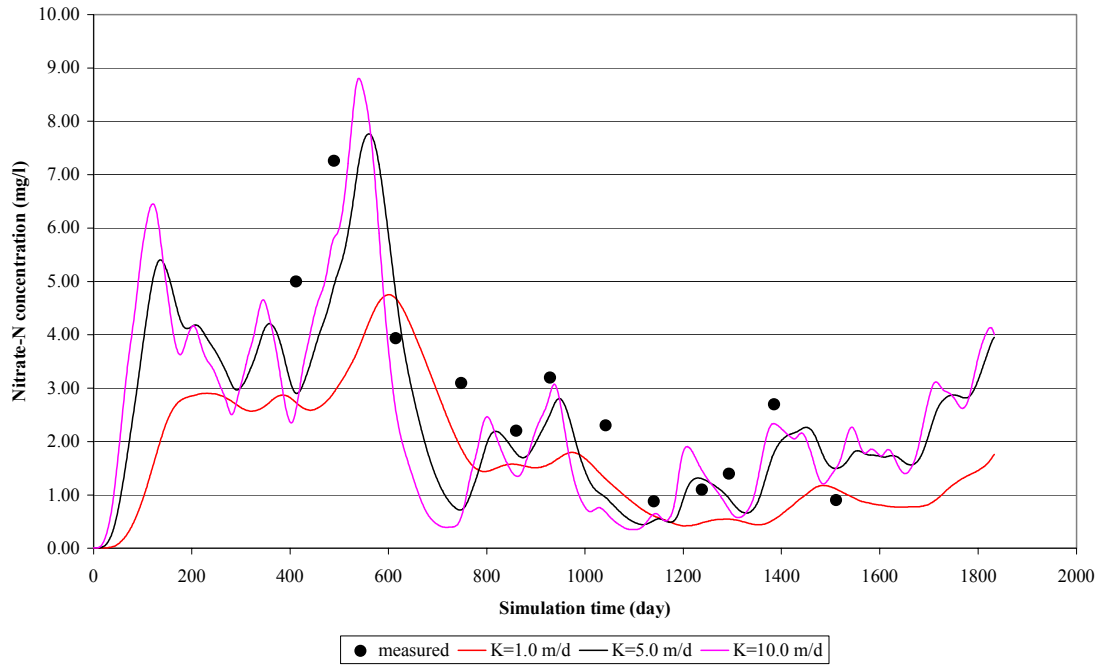


Figure 5: Comparison between measured and simulated BTCs at monitoring well 2

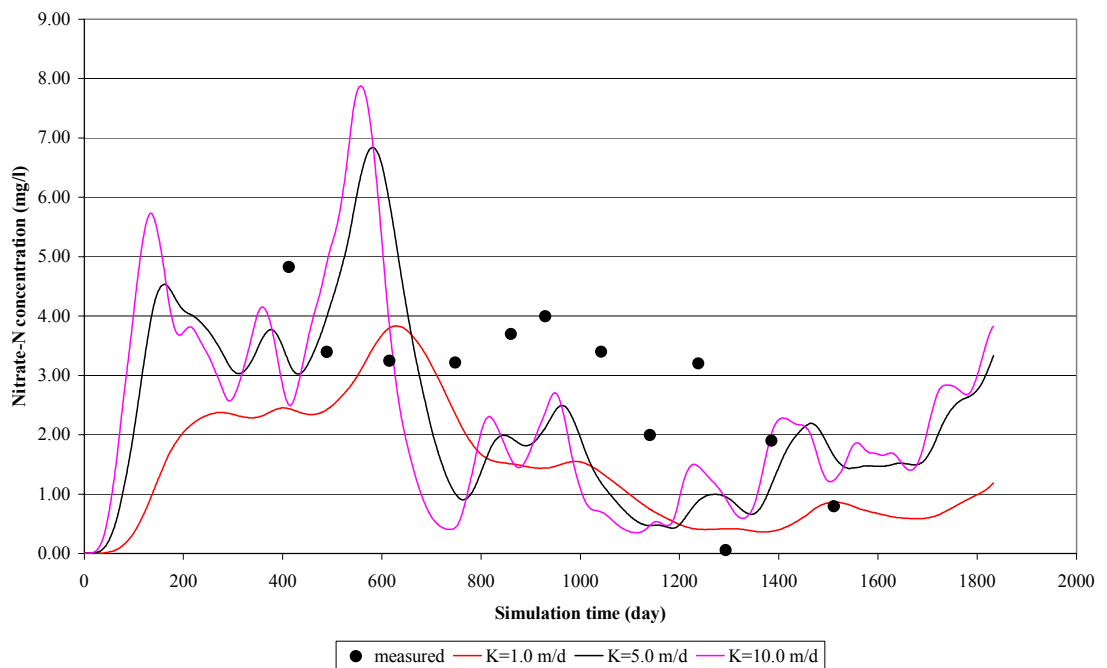


Figure 6: Comparison between measured and simulated BTCs at monitoring well 3

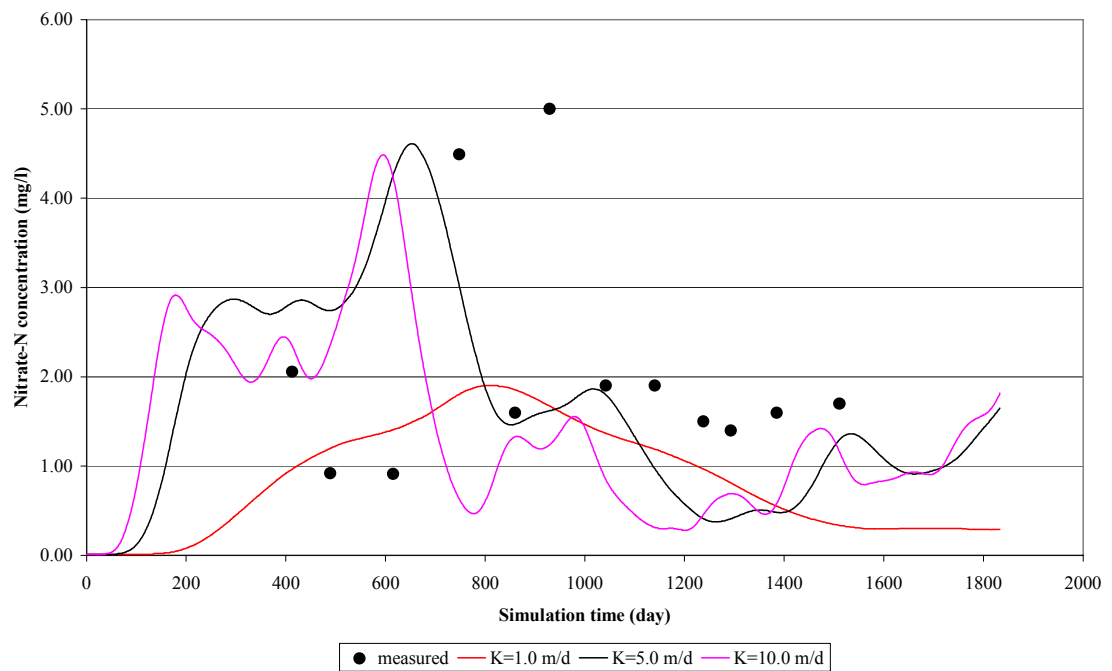


Figure 7: Comparison between measured and simulated BTCs at monitoring well 4

Overall, the model with a hydraulic conductivity of 5.0 m/day was able to fit the measured nitrate-N concentrations best. The relatively long time between samplings resulted in the dynamics of the simulated values not being able to be fully verified by field measurements.

6 ACACIA BAY SBR MODEL CALIBRATION

The target of our model calibration was that the predicted concentration peaks at monitoring wells 1 and 2 should be as close to those measured, while the root-mean-squares (RMS) residual errors between measured and simulated nitrate-N concentrations at all monitoring wells (monitoring wells 1 to 4 and control well) are minimised. The calibrated parameter values are shown in Table 1, along with the range over which they were investigated. Comparisons between measured and simulated break through curves (BTCs) at all monitoring wells are shown in Figure 3 to Figure 7.

Table 1: Calibrated parameters for Acacia Bay SBR model and range over which they were investigated

| Parameter | Calibrated value | Investigated range | Source |
|--|-------------------------|---------------------------|--|
| Hydraulic conductivity (m/day) | 5.0 | 1-10 | Calibrated |
| Maximum rate of denitrification (mg/l/day) | 0.1 | 0.01-0.2 | Calibrated |
| Rate constant of nitrification (/day) | 0.01 | 0.005-0.1 | Calibrated |
| Longitudinal dispersivity (m) | 5.0 | 2.5-10.0 | Calibrated |
| Horizontal transverse dispersivity (m) | 1.0 | 0.5-2.0 | Calibrated |
| Vertical transverse dispersivity (m) | 0.1 | 0.05-0.2 | Fixed at 10% of horizontal transverse dispersivity |

7 ACACIA BAY SBR MODEL SENSITIVITY ANALYSIS

The sensitivity of simulated BTCs at monitoring wells to the unmeasured model parameters was investigated.

7.1 Hydraulic Conductivity

This effect of varying hydraulic conductivity between 1, 5 and 10 m/day is shown in Figure 3 to Figure 7.

In the closest well (number 1), there is very little difference between the simulated nitrate-N concentrations for all three values of hydraulic conductivity. This occurs because of the short distance between this monitoring well and the source of the nitrate-N in the SBR discharge trenches. Due to the short distance, the effect of various hydraulic conductivities on the travel speed and transformations on the nitrate-N has very little opportunity to express itself upon the simulated nitrate-N concentrations. As distance gets greater, as in wells 2 to 4, there are larger differences between the three simulated values. The simulated values with the higher conductivities are more dynamic in terms of the predicted nitrate-N concentrations and reflect more closely the input dynamics of the discharging effluent. The hydraulic conductivity of 5.0 m/day is considered to provide the best fit to the measured nitrate-N peaks at monitoring wells 1 and 2 and lowest root-mean-squares (RMS) residual errors between measured and simulated nitrate-N concentrations at all monitoring wells.

The hydraulic conductivity of 5.0 m/day is somewhat greater, but still consistent, with the average value measured from slug tests in three monitoring wells (wells 1 to 3) of 1.6 m/day (Table 2) (Hadfield and Piper, 2005). The reason that the calibrated value is higher is probably due to spatial variability in the aquifer. The measured concentration data is a reflection of the upstream aquifer characteristics and nutrient transformations, whereas the slug data is considered to be a point source measurement reflecting aquifer characteristics only at the point of measurement. The measured hydraulic conductivity data varied over two orders of magnitude, so agreement of the measured 1.6 m/day to the effective calibrated hydraulic conductivity of 5.0 m/day is not unreasonable.

Table 2: *Acacia Bay slug test data (Hadfield and Piper, 2005)*

| Monitoring well | Conductivity (m/day) |
|---------------------------|----------------------|
| Well 1 | 0.054 |
| Well 2 | 3.84 |
| Well 3 | 0.945 |
| Arithmetic average | 1.61 |

7.2 Rate of Denitrification

The effect of denitrification on nitrate-N concentrations in the control well and monitoring wells 1 to 4 is shown in Figure 8 to Figure 12, respectively. The hydraulic conductivity is assumed to be the calibrated value of 5 m/day.

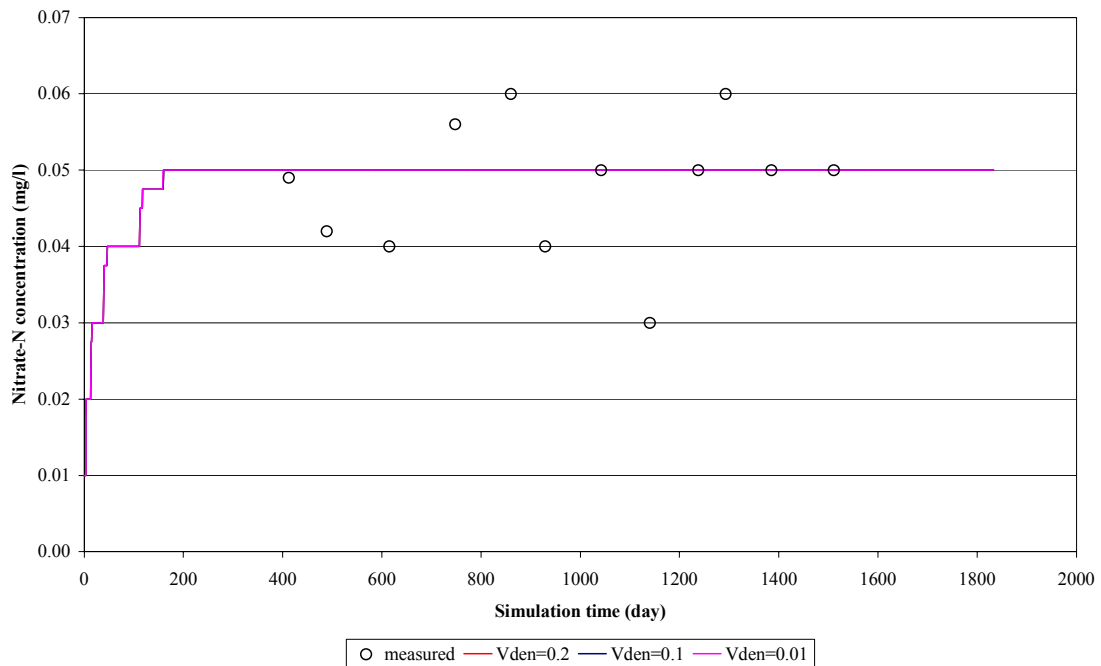


Figure 8: Simulated BTC at the control well as affected by the rate of denitrification (V_{den}). Results for $V_{den}=0.2$ and 0.1 are plotted under the $V_{den}=0.01$ line.

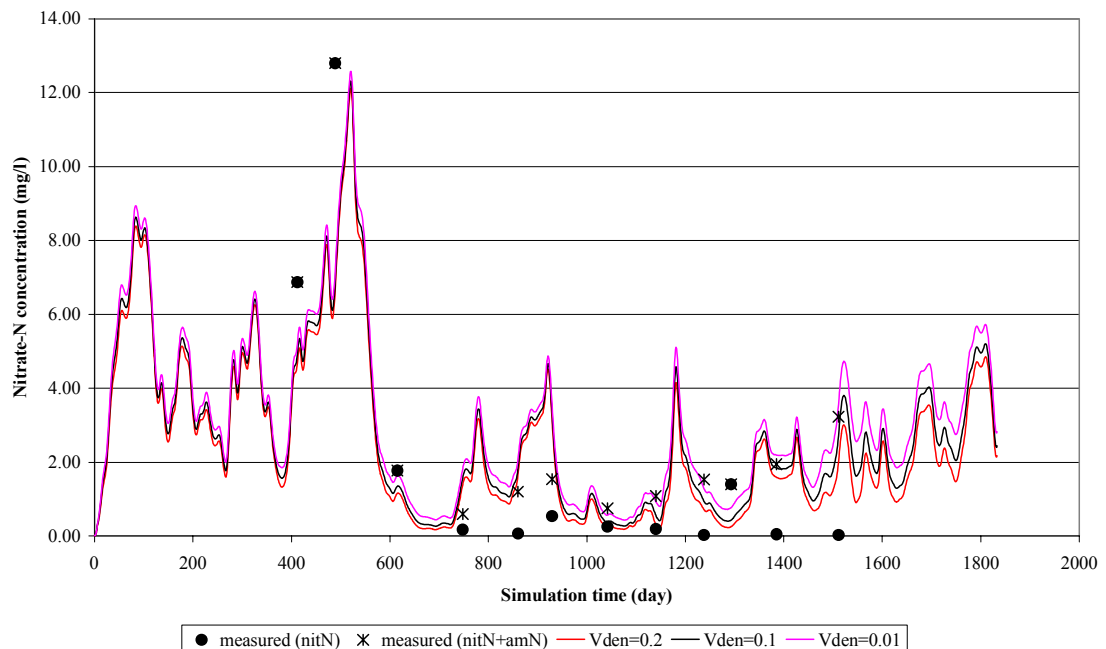


Figure 9: Simulated BTC at monitoring well 1 as affected by the rate of denitrification (V_{den})

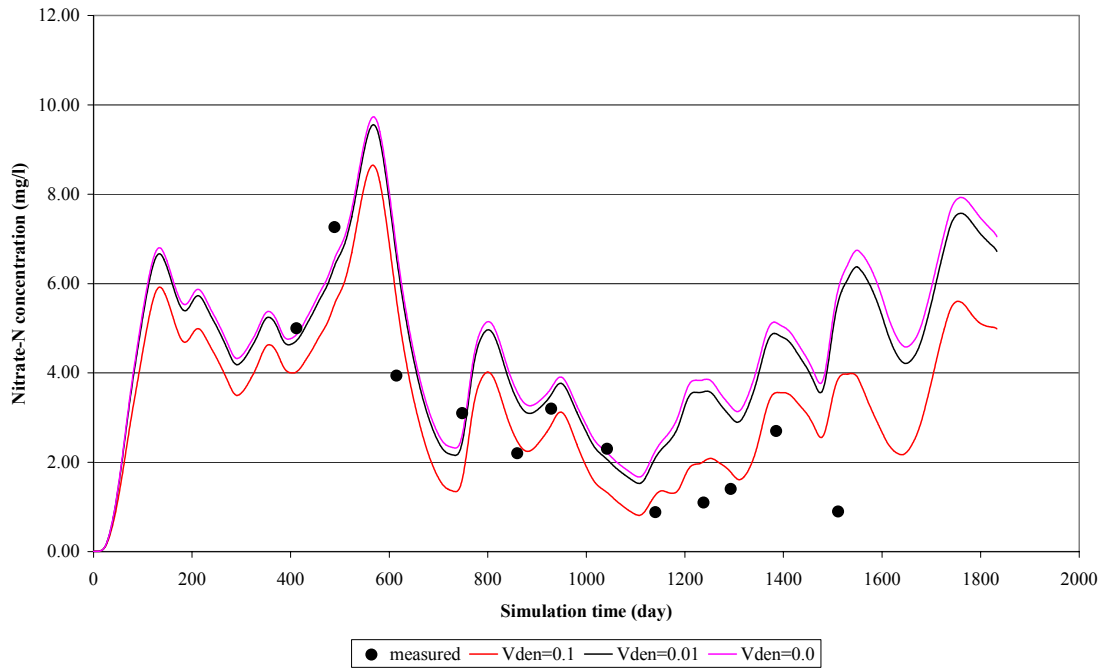


Figure 10: Simulated BTC at monitoring well 2 as affected by the rate of denitrification (V_{den})

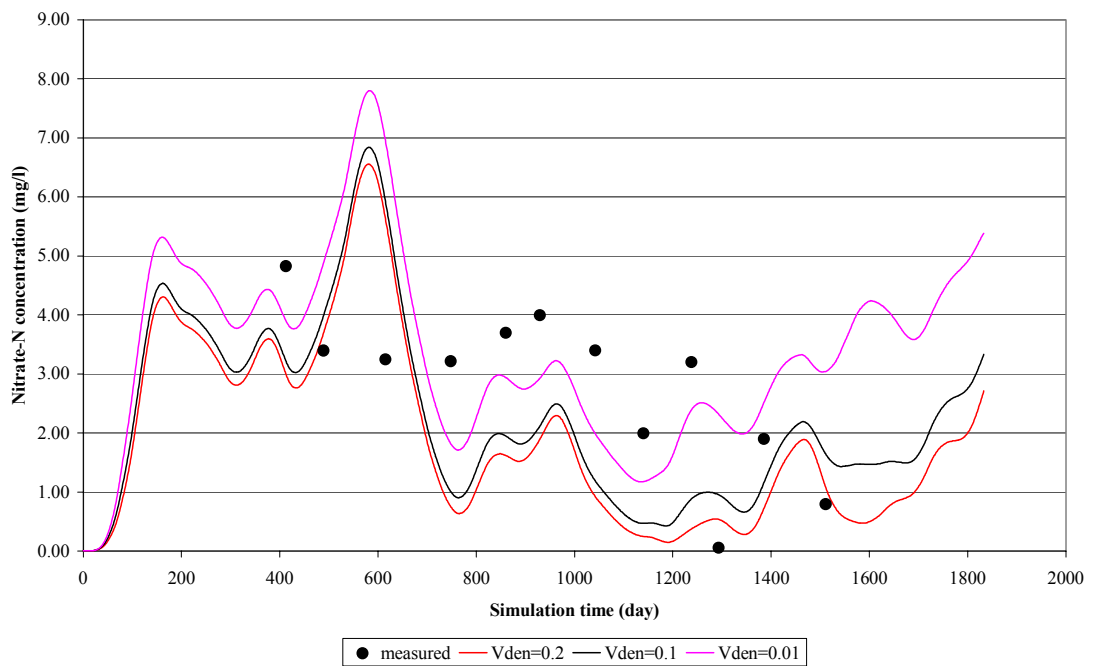


Figure 11: Simulated BTC at monitoring well 3 as affected by the rate of denitrification (V_{den})

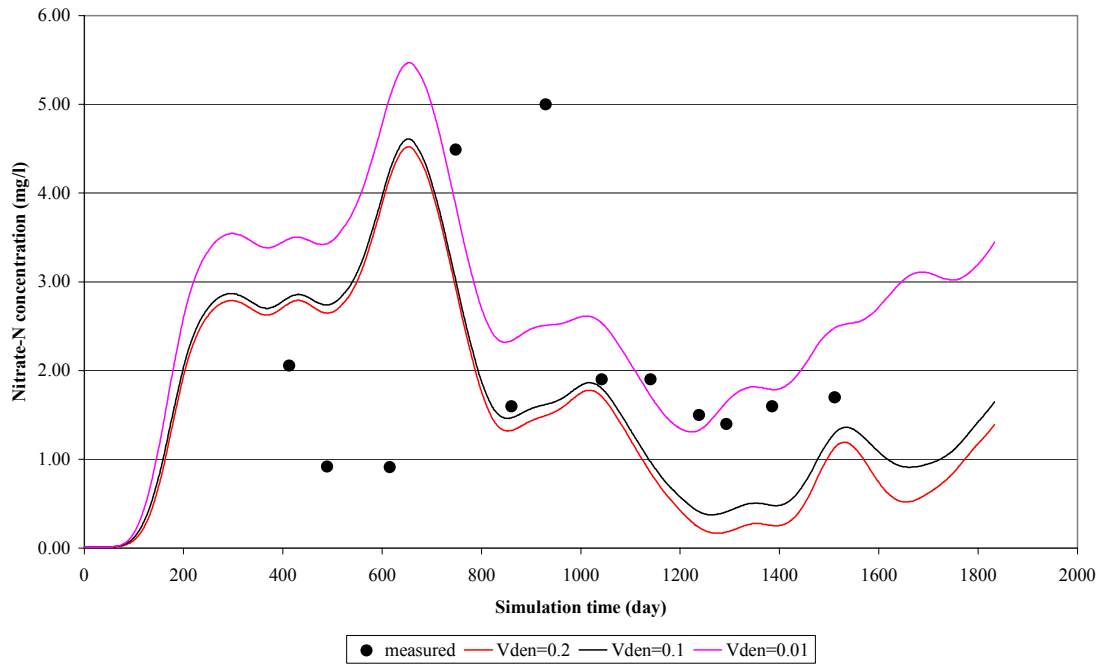


Figure 12: Simulated BTC at monitoring well 4 as affected by the rate of denitrification (Vden)

The effect of the rate of denitrification on the simulated nitrate-N concentration increases with distance (or time) from the effluent source. With greater time, the effect of a higher rate of denitrification has more opportunity to effect the resulting concentration of nitrate-N. The denitrification rate of 0.1 mg/l/d gave the overall best fit to the monitoring data.

7.3 Rate of Nitrification

The effect of nitrification on nitrate-N concentrations in the control well and the four monitoring wells is shown in Figure 13 to Figure 17.

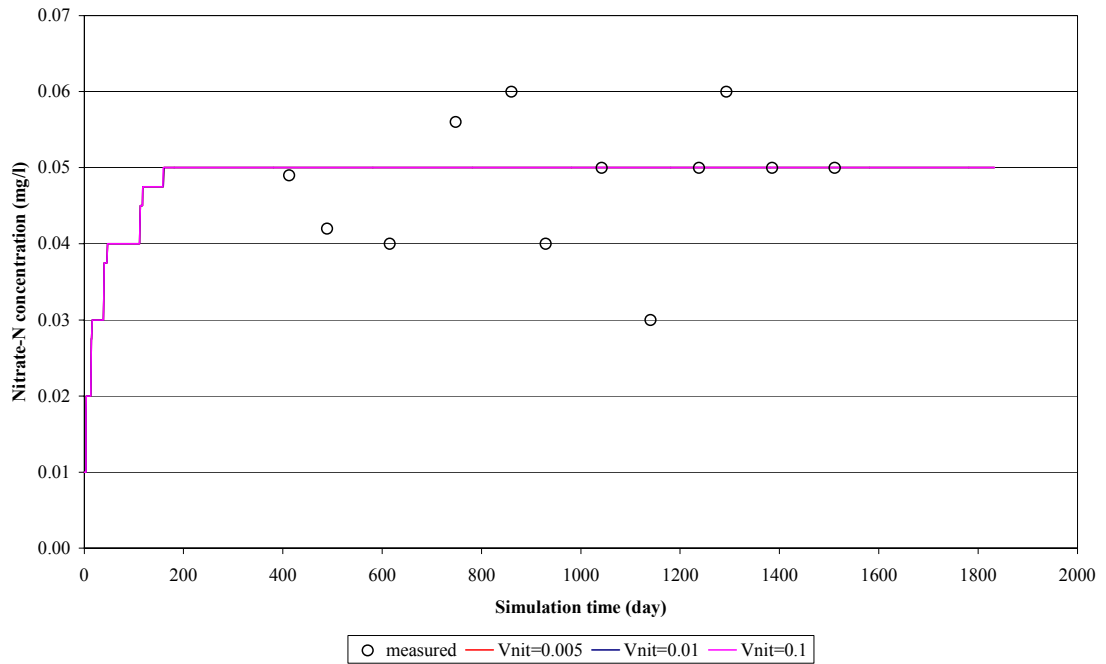


Figure 13: Simulated BTC at the control well as affected by the rate of nitrification (V_{nit}). Results for $V_{nit}=0.005$ and 0.01 plotted under the $V_{nit}=0.1$ per day.

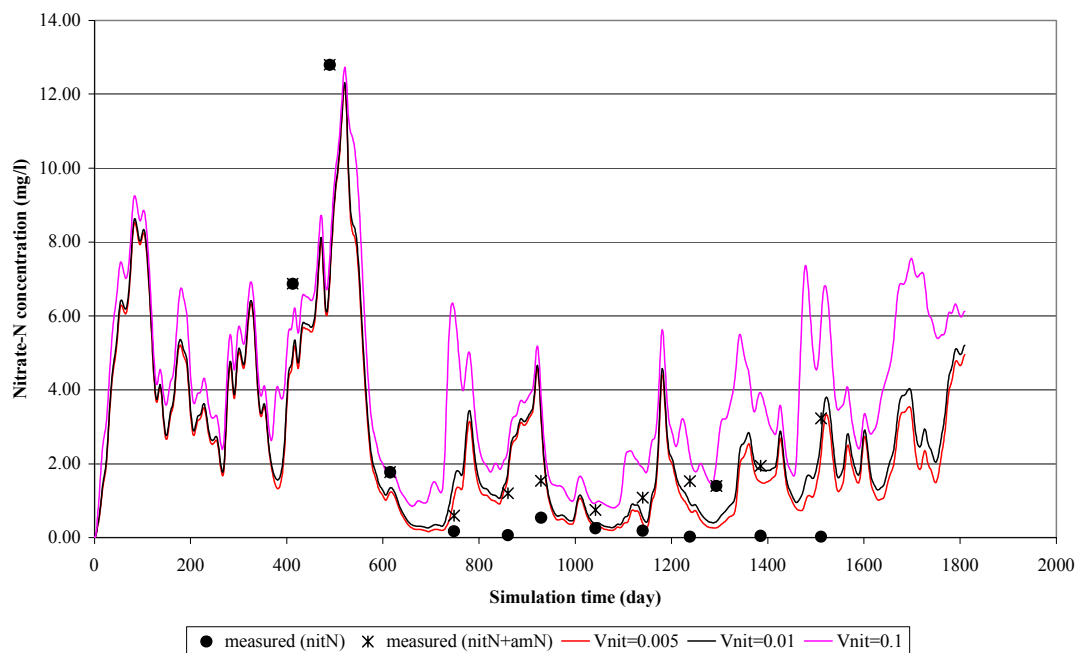


Figure 14: Simulated BTC at monitoring well 1 as affected by the rate of nitrification (V_{nit})

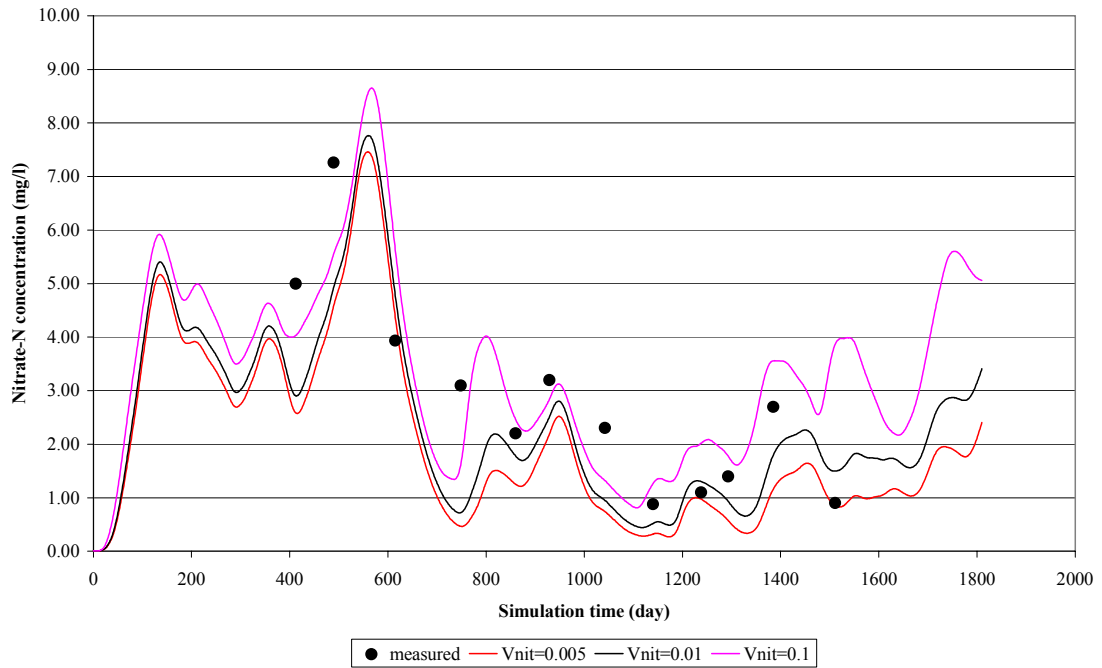


Figure 15: Simulated BTC at monitoring well 2 as affected by the rate of nitrification (V_{nit})

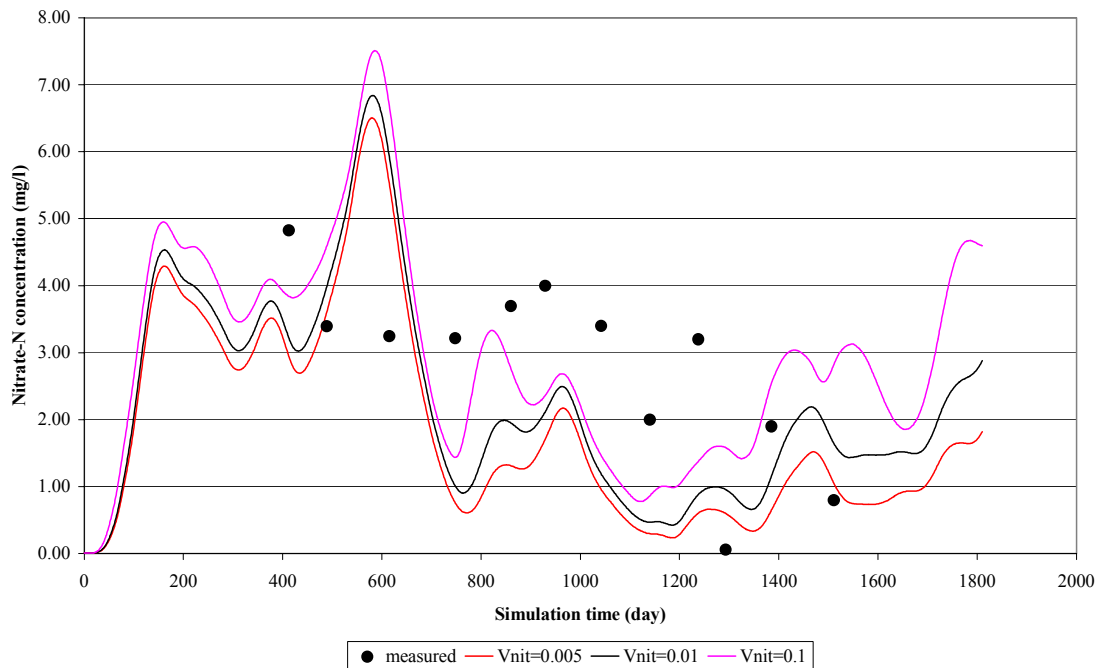


Figure 16: Simulated BTC at monitoring well 3 as affected by the rate of nitrification (V_{nit})

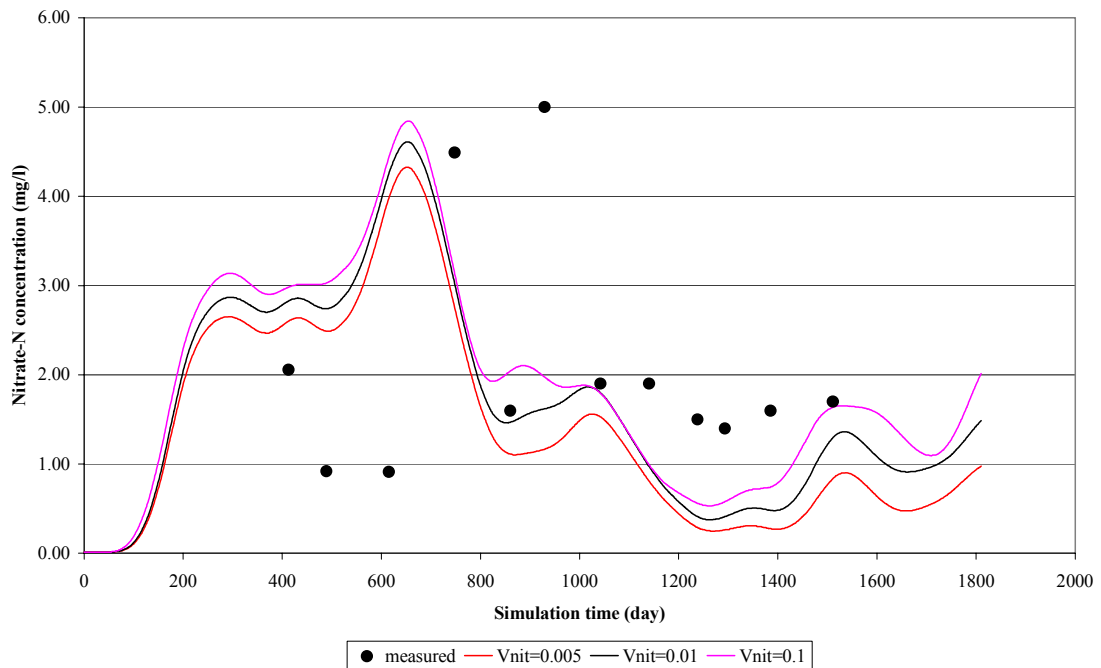


Figure 17: Simulated BTC at monitoring well 4 as affected by the rate of nitrification (V_{nit})

The effect of the rate of nitrification on the nitrate-N concentration is dependant not only on the parameter describing this conversion reaction (V_{nit}) but also the mass of ammonia present at that location in the model domain. The difference between the three parameter rates is greatest in well 1, which is closest to the discharging trench, and also where the ammonia concentrations were the highest.

7.4 Dispersion Coefficient

The longitudinal dispersivity was not particularly sensitive parameter in most monitoring wells, as can be seen in Figure 18 to Figure 22. A longitudinal dispersivity value of 5.0 m was the parameter, which gave the best fit to the measured nitrate-N data. The horizontal transverse dispersivity was taken to be 20% of the longitudinal dispersivity, while the vertical transverse dispersivity was 0.1 m, which is 10% of the horizontal transverse dispersivity (Zheng and Bennett, 1995).

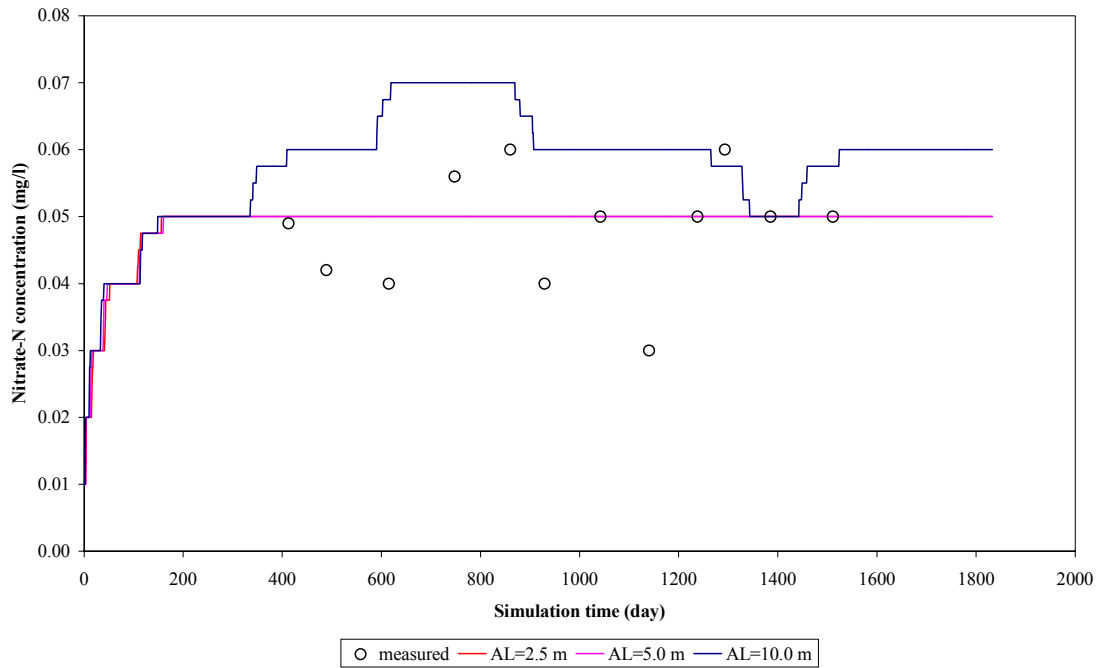


Figure 18: Simulated BTC at the control well as affected by longitudinal dispersivity (AL)

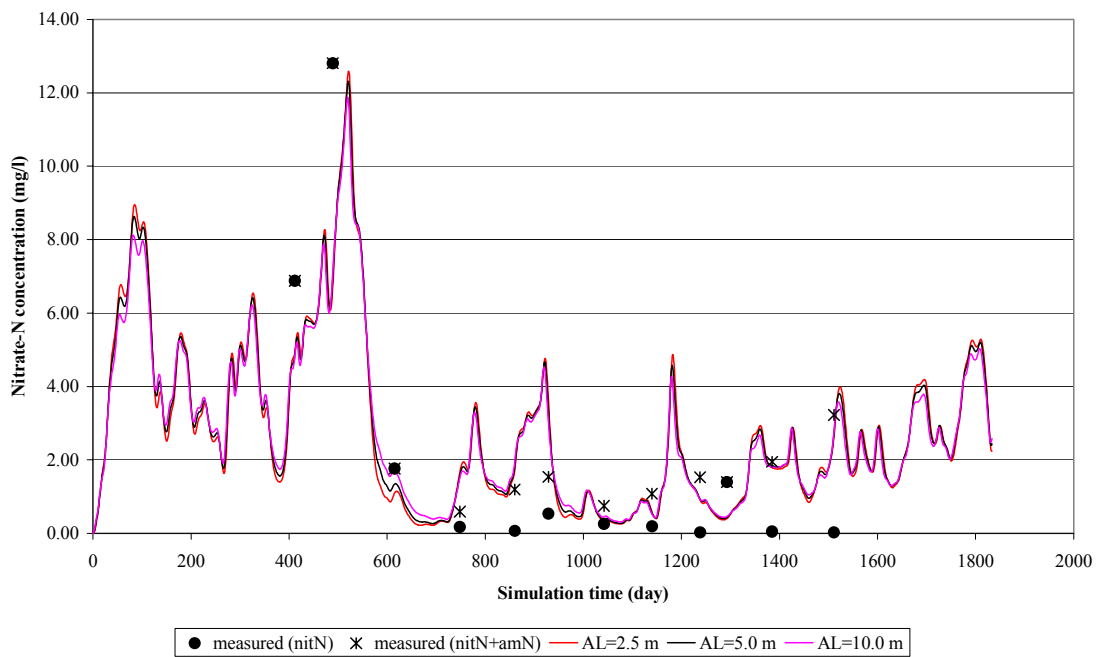


Figure 19: Simulated BTC at monitoring well 1 as affected by longitudinal dispersivity (AL)

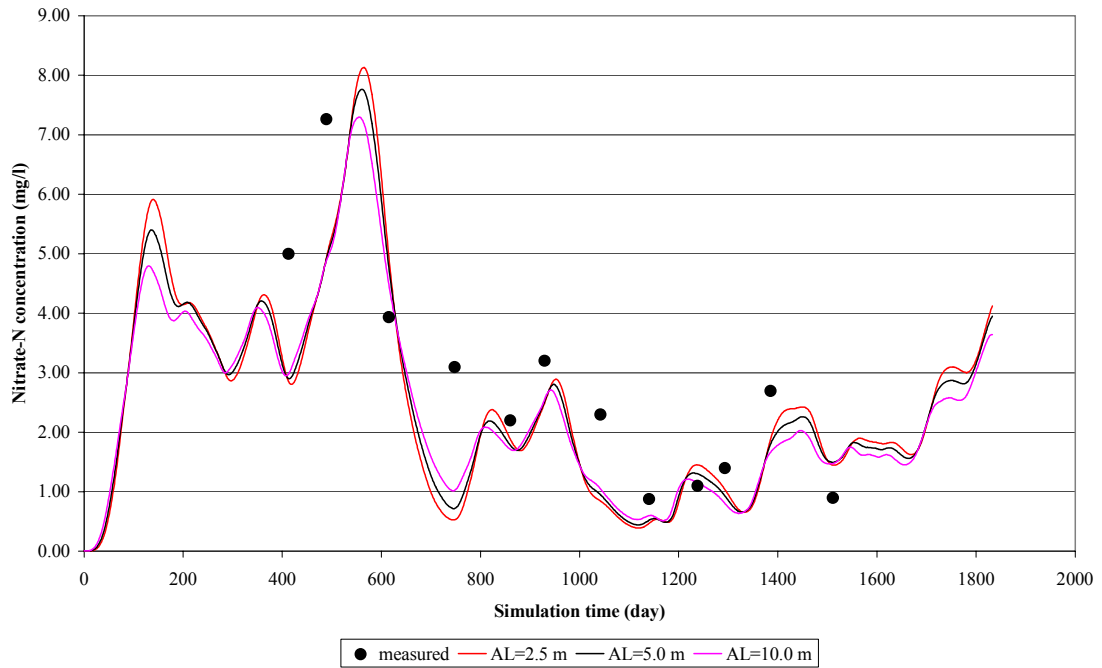


Figure 20: Simulated BTC at monitoring well 2 as affected by longitudinal dispersivity (AL)

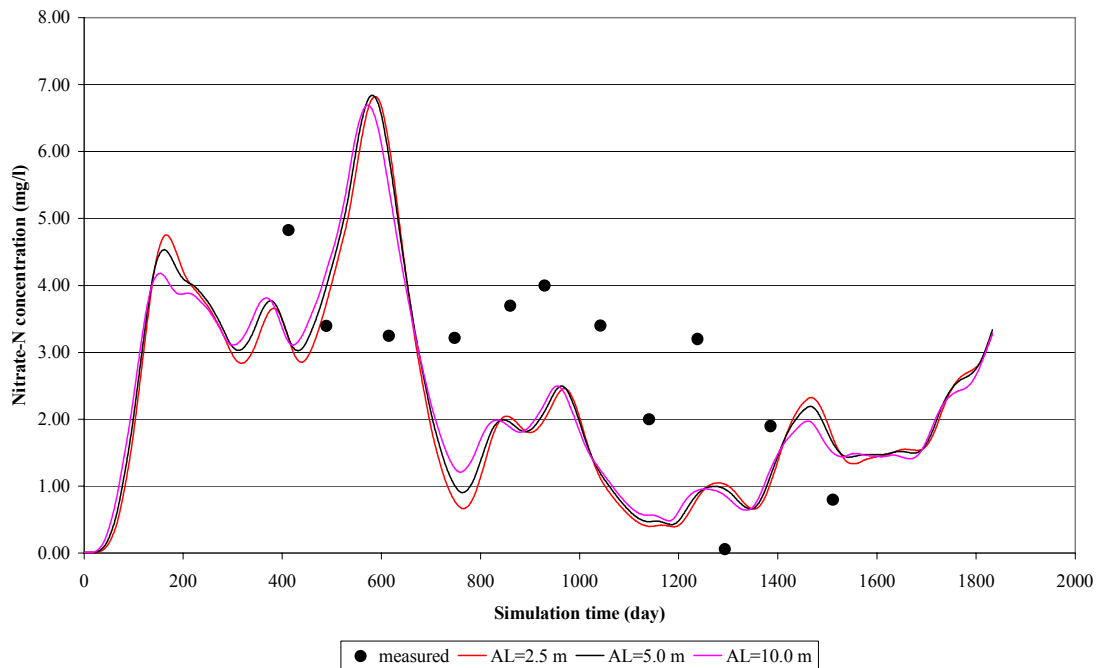


Figure 21: Simulated BTC at monitoring well 3 as affected by longitudinal dispersivity (AL)

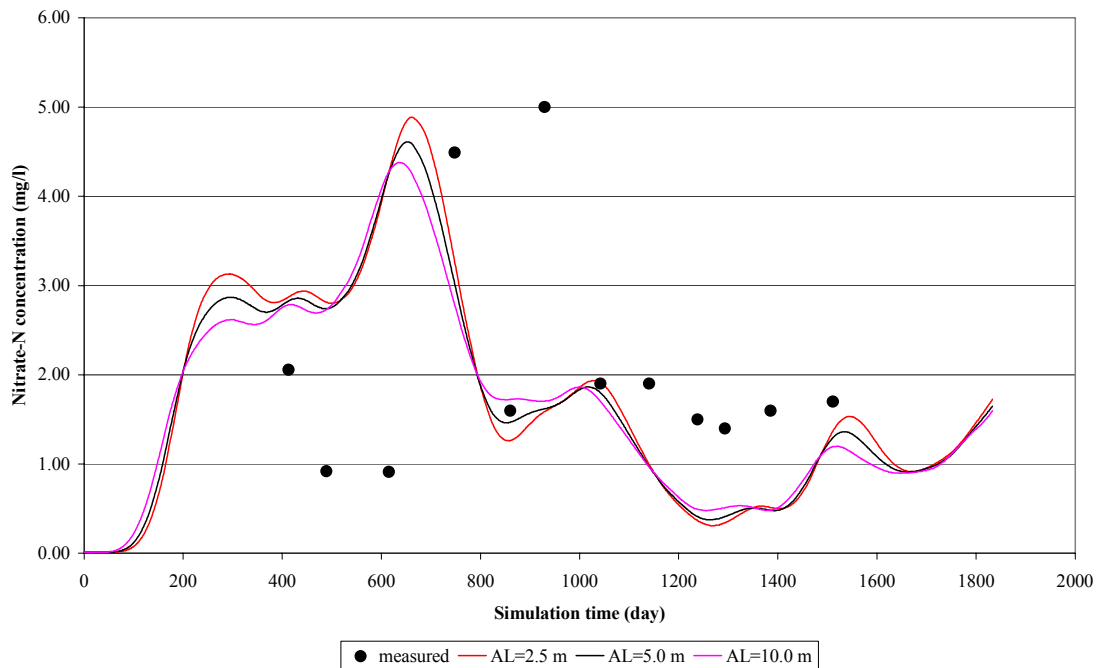


Figure 22: Simulated BTC at monitoring well 4 as affected by longitudinal dispersivity (AL)

7.5 Spatial Variation in Hydraulic Conductivity

Since the actual aquifer might be heterogeneous in hydraulic properties, especially in hydraulic conductivity, Monte Carlo numerical simulations were conducted by using 40 equally possible descriptions of the hydraulic conductivity field. These fields were generated by the multiple indicator conditional stochastic simulation (MICSS) technique (Gomez-Hernandez and Srivastava, 1990). We used seven indicators to represent hydraulic conductivity values of 1, 2, 3, 5, 7, 8, and 9 m/day, respectively. It is assumed that the semivariogram model is exponential without nugget in the form of:

$$\gamma(h) = s \left[1 - \exp \left(- \frac{|h|}{\lambda} \right) \right]$$

Where:

- s is the sill,
- λ is the correlation scale, and
- h is lag.

We assumed that the correlation scale and sill are 25 m and 0.15 in the horizontal direction, and 5 m and 0.25 in the vertical direction. Simulated BTCs at each of the four monitoring wells downstream of discharge trenches are shown against measured BTCs in Figure 23. Although not all measured nitrate-N concentrations are in the concentration ranges predicted by Monte Carlo simulations, significant improvement of prediction has been achieved. This implied that actual aquifer may have a much larger variance of logarithm hydraulic conductivity than the value used here (0.125).

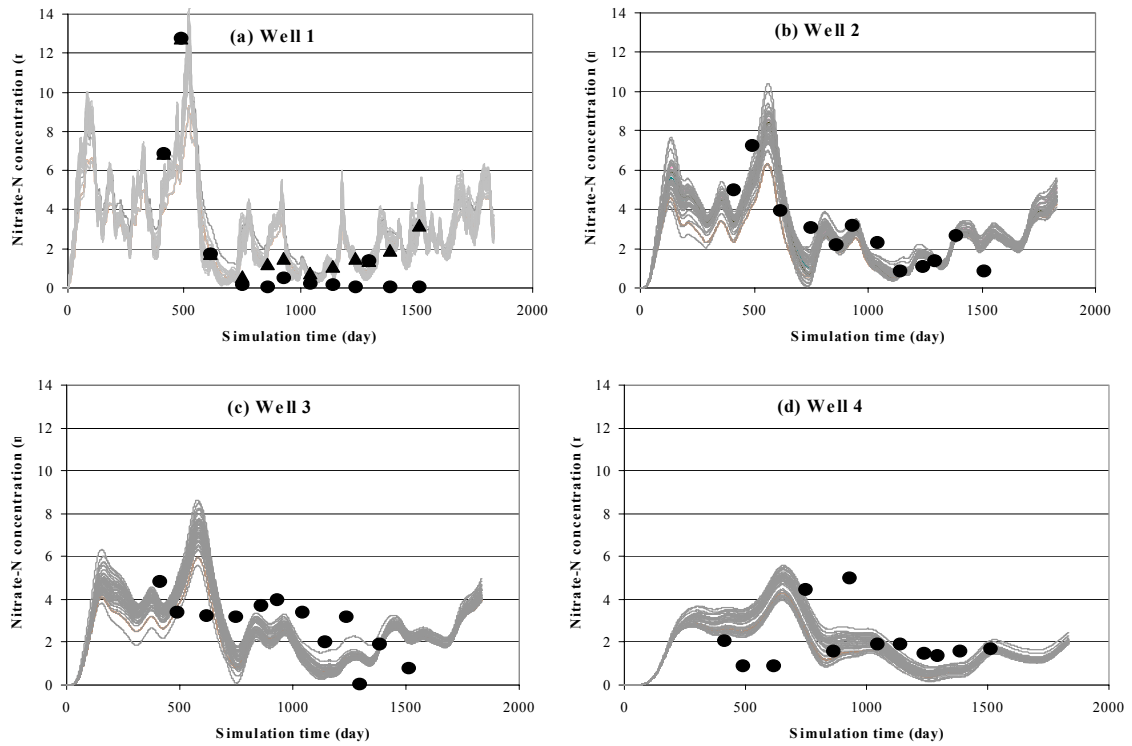


Figure 23: Monte Carlo simulated BTCs (lines) compared with measured BTCs at monitoring wells (dots)

8 MONITORING DATA AND SITE LAYOUT OF KINLOCH SBR DISCHARGE

The reader is referred to Barkle (2004) for a full description of the Kinloch SBR site, trench locations, and monitoring wells and data.

9 KINLOCH SBR MODEL SETUP AND INPUT DATA

The model domain for the Kinloch SBR model is 600 m long, 200 m wide and 50 m high (Figures 24a and 24b), and was divided into 17 numerical layers. The thickness of numerical layers increases from 1 m in the zone near top boundary to 6 m in the zone near bottom boundary. The discharge trench, 81 m long and 2.5 m wide, was aligned in the groundwater flow direction (X-coordinate), and was located in the middle of the Y-coordinate and 200 m away from the upstream boundary. The bottom of the trench was treated as a specified flux boundary with weekly measured effluent discharge data as input. A uniform rainfall recharge rate was applied to the area of the top boundary, except for the area covered by the trench. Each numerical layer was divided into 588 numerical elements. Upstream and downstream boundary conditions are specified as constant heads. The groundwater head is 41 m and 39.8 m respectively at the upper and lower boundaries. The distance between the upper and lower boundary is 600 m and thus hydraulic gradient is 0.2%. The numerical mesh is dense inside the discharge trench and its surrounding area. The discharge trench was divided into 27 elements of the size of 9 m long and 0.833 m wide.

The improvements in this Kinloch SBR model from that developed by previous work (Barkle and Wang, 2003) include:

- Upstream nitrate-N concentration based on measured data in the control well;
- Hydraulic gradient based on measured data (0.2%);
- Effluent input based on weekly samplings;
- Better resolution of the finite element grid; and
- Simulated nitrate-N concentrations based on average concentrations over the screened depth of the monitoring wells.

The model parameters that were not initially measured in this study included:

- Saturated hydraulic conductivity (later measured);
- Nitrification rate;
- Denitrification rate;
- Horizontal dispersivity;
- Horizontal transverse dispersivity; and
- Vertical transverse dispersivity.

These parameters, except the vertical transverse dispersivity, which is fixed at 10% of the horizontal transverse dispersivity, were calibrated and a sensitivity analysis of these parameters was undertaken.

At this site the SBR discharge trench was no longer used for disposal of effluent after day 1400. A denitrification bed and discharge field away from this site was used after this date. The initial nitrate-N concentration and nitrate-N concentration of the incoming water from upstream boundary are 3.5 mg/l, based on measured data at monitoring well 1 (control well). The rate of water drainage from top soils and nitrate-N concentration of drainage water were set at 1 mm/day (Hadfield, 1995) and 2.2 mg/l, respectively.

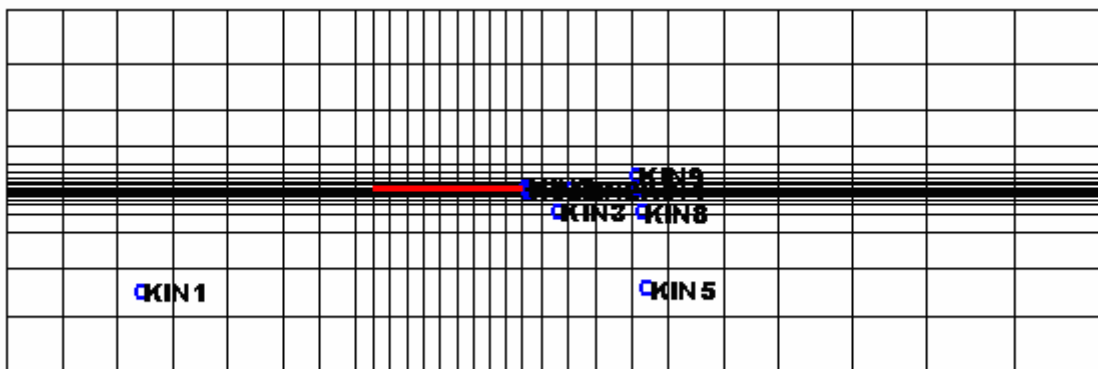


Figure 24(a): Plan view of the numerical mesh, locations of effluent discharge trench (rectangle in red colour) and monitoring wells (dots) for the Kinloch SBR model.

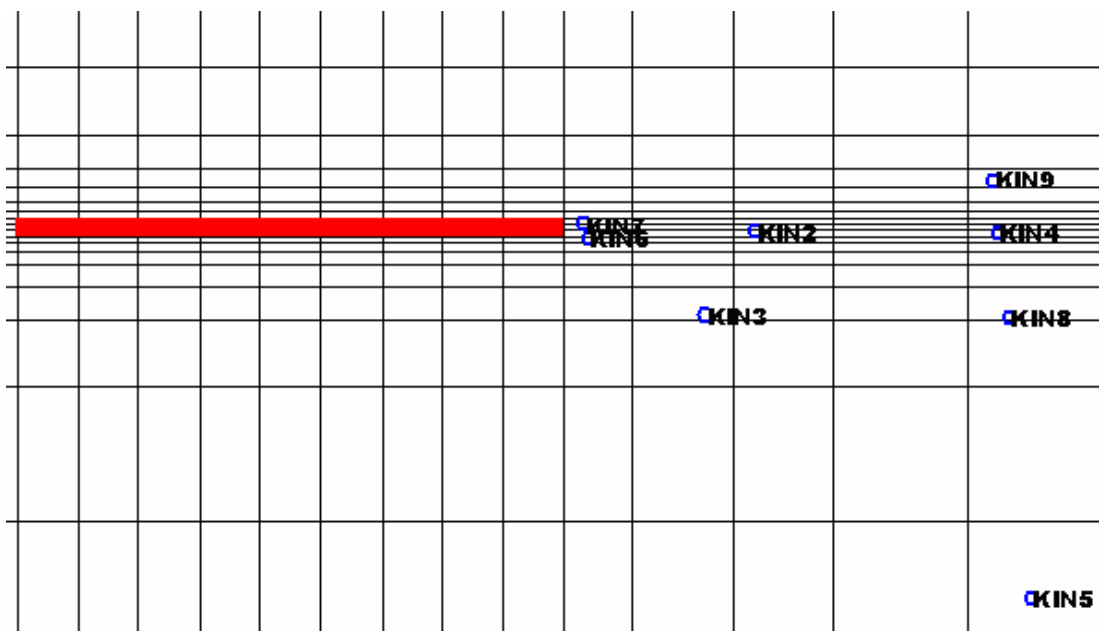


Figure 24(b): Locations of sampling wells at the Kinloch site (sampling well 1 not shown). Rectangle represents discharge trench and circles represent wells.

While the domain is discretised into rectangular elements for optimum speed in the solution to the particle tracking equations for the solute transport, the simulation is still a finite element scheme.

10 ANALYSES OF MEASURED NITRATE-N CONCENTRATIONS AT KINLOCH SBR MONITORING WELLS

As is shown in Figure 25, two large nitrate-N concentration peaks occurred in the discharging effluent during the simulation period. Observed BTCs at monitoring wells 1 (control) and 5 (Figure 26 and Figure 27) showed no obvious nitrate-N concentration peaks, meaning that nitrate-N concentration at these two wells were not significantly affected by effluent discharge.

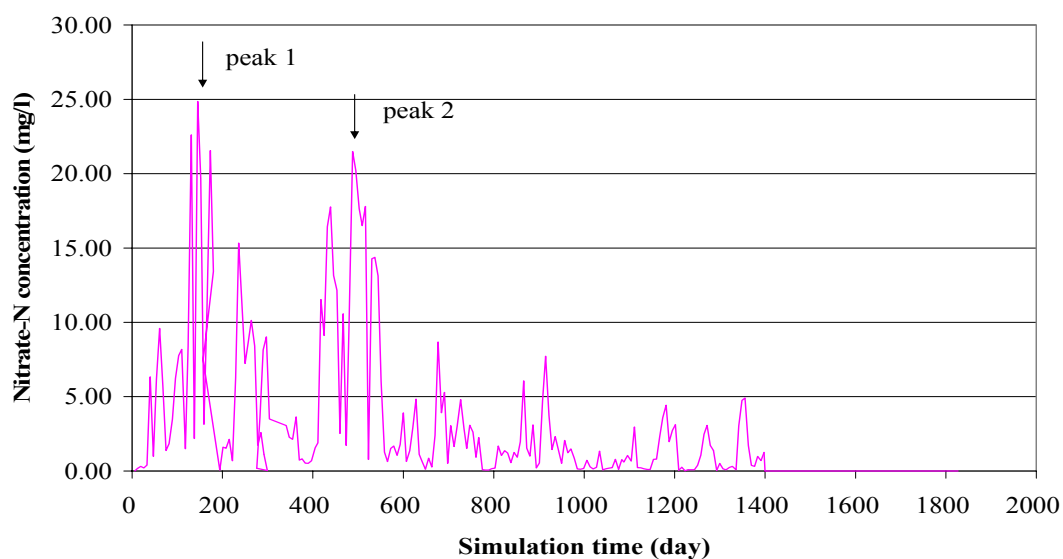


Figure 25: Nitrate-N concentration of discharged effluent vs simulation time

The average nitrate-N concentrations in wells 1 and 5, over the monitoring period, were 3.1 and 2.8 mg l⁻¹ NO₃-N, respectively. It has been shown that these wells are outside of the SBR contaminate plume (Barkle, 2004). However, these nitrate-N concentrations are higher than what would be expected for uncontaminated groundwater within the Taupo catchment. For example, at Acacia Bay the control well has a mean nitrate concentrations of less than 0.05 mg l⁻¹ NO₃-N. A publication on the history of Kinloch (Kinloch, 1998) shows an old woolshed and associated stock yards were located in this vicinity. It is conceivable that these elevated nitrate levels in these two wells are due to contamination from this historical point source of animal effluent. Hadfield and Barkle (2004) have shown that the nitrate loading from woolsheds and yards can be as high as 1000 kg N/yr.

Monitoring wells 6 to 9 are located directly downstream of the discharge trench, but no nitrate-N concentration peaks were detected at these wells due to samples not being collected at these wells until day 1329 of the simulation (Figure 28 and Figure 29, and Figure 33 and Figure 34). Samples were collected from wells 1 to 5 from day 411. Observed BTCs at monitoring wells 2 and 3 (Figure 30 and Figure 31), which are very close to the discharge trench, showed only one nitrate-N concentration peak on the day 614. This means that the first nitrate-N peak had already passed these monitoring wells by the time the first sample was collected on day 411. Monitoring

well 4 is the only well for which the two nitrate-N concentration peaks were observed; on day 411 and day 744. These two peaks were observed in well 4 as this well was further downstream of the trench than wells 2 and 3 (Figure 32).

Assuming that the peak concentration data is valid, it is possible to estimate the average pore velocity at the site, based on the differences between the time of peak concentrations in the monitoring wells and the discharge trench (Table 3). These pore velocities showed only small variations, with an average value of 0.46 m/day. Assuming a porosity value of 0.3, the average Darcy velocity is 1.53 m/day. Based on gradient data (Figure 18; Barkle, 2004) the hydraulic gradient around the discharge trench is not likely to be over 4.5%. Therefore, the hydraulic conductivity is likely to be higher than 34 m/day ($1.53/0.045$). This estimated value from gradient and peak nitrate-N concentrations is over 37 times larger than the average measured hydraulic conductivity of 0.9 m/day (Table 4). It is possible that the monitoring wells were not developed sufficiently to enable the slug tests to reflect the true hydraulic conductivity of the aquifer.

Table 3: Estimation of pore water velocity based on nitrate-N peaks in monitoring wells

| | Distance to SBR trench (m) | Peak time (day) | | Peak time difference (day) | | Pore velocity (m/day) | |
|----------------|----------------------------|-----------------|--------|----------------------------|--------|-----------------------|--------|
| | | Peak 1 | Peak 2 | Peak 1 | Peak 2 | Peak 1 | Peak 2 |
| Trench | | 145 | 489 | | | | |
| Well 2 | 68.5 | - | 614 | - | 125 | - | 0.55 |
| Well 3 | 60.3 | - | 614 | - | 125 | - | 0.48 |
| Well 4 | 104.2 | 411 | 744 | 266 | 255 | 0.39 | 0.41 |
| Average | | | | | | 0.46 | |

Table 4: Kinloch slug test data (Hadfield and Piper, 2005)

| Monitoring well | Conductivity (m/day) |
|------------------------|----------------------|
| Well 6 | 0.21 |
| Well 7 | 2.11 |
| Well 8 | 1.18 |
| Well 9 | 0.19 |
| Arithmetic mean | 0.92 |

11 KINLOCH SBR MODEL CALIBRATION

The target of the model calibration is similar to that of the Acacia Bay modelling exercise (Section 4), where the concentration peaks at monitoring wells 2 to 4 are predicted and the root-mean-squares (RMS) residual errors between measured and simulated nitrate-N concentrations at all monitoring wells (wells 1 to 9) are minimised. Calibrated model parameter values are shown in Table 5.

Table 5: Calibrated parameters for Kinloch SBR model and range over which they were investigated

| Parameter | Calibrated value | Range investigated |
|--|------------------|--------------------|
| Hydraulic conductivity (m/day) | 150.0 | 1-200 |
| Maximum rate of denitrification (mg/l/day) | 1.0 | 0.01-2.0 |
| Rate constant of nitrification (/day) | 0.01 | 0.005-0.1 |
| Longitudinal dispersivity (m) | 5.0 | 0.5-10.0 |
| Horizontal transverse dispersivity (m) | 1.0 | 0.1-2.0 |
| Vertical transverse dispersivity (m) | 0.1 | 0.01-0.2 |

Comparisons between measured and simulated BTCs at all monitoring wells are shown in **Error! Reference source not found.** to Figure 33. Also shown in these figures are the simulation results using the average hydraulic conductivity value obtained from slug tests (1 m/day, Table 4), the value estimated from peak concentration times (40 m/day) and higher values of 150 m/day and 200 m/day.

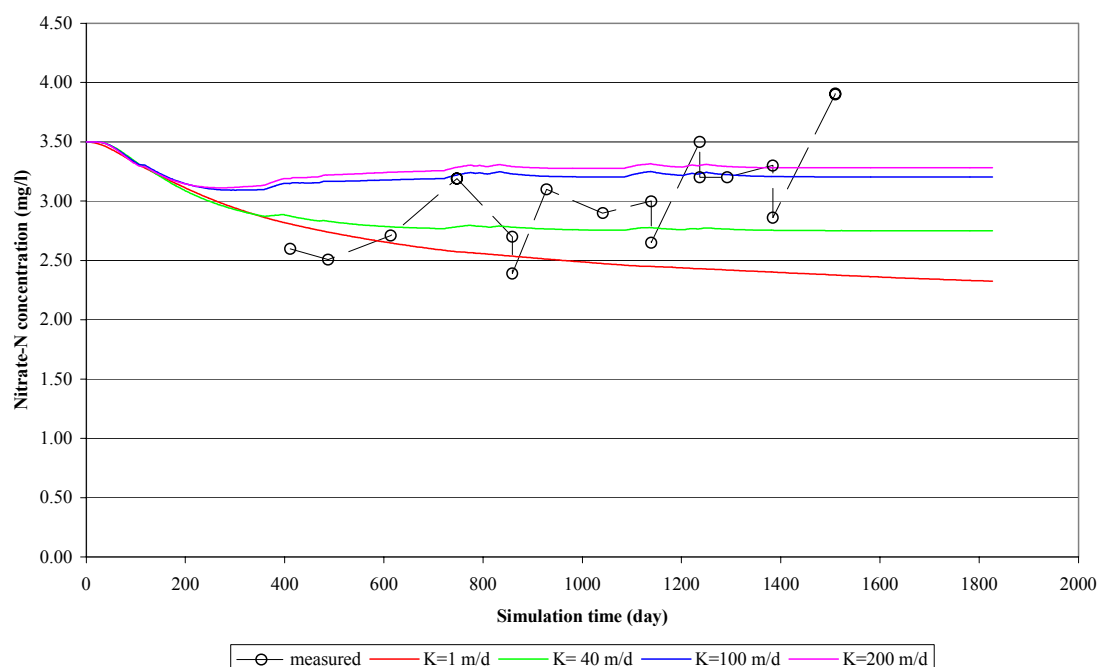


Figure 26: Comparison between measured and simulated BTCs at monitoring well 1 (control)

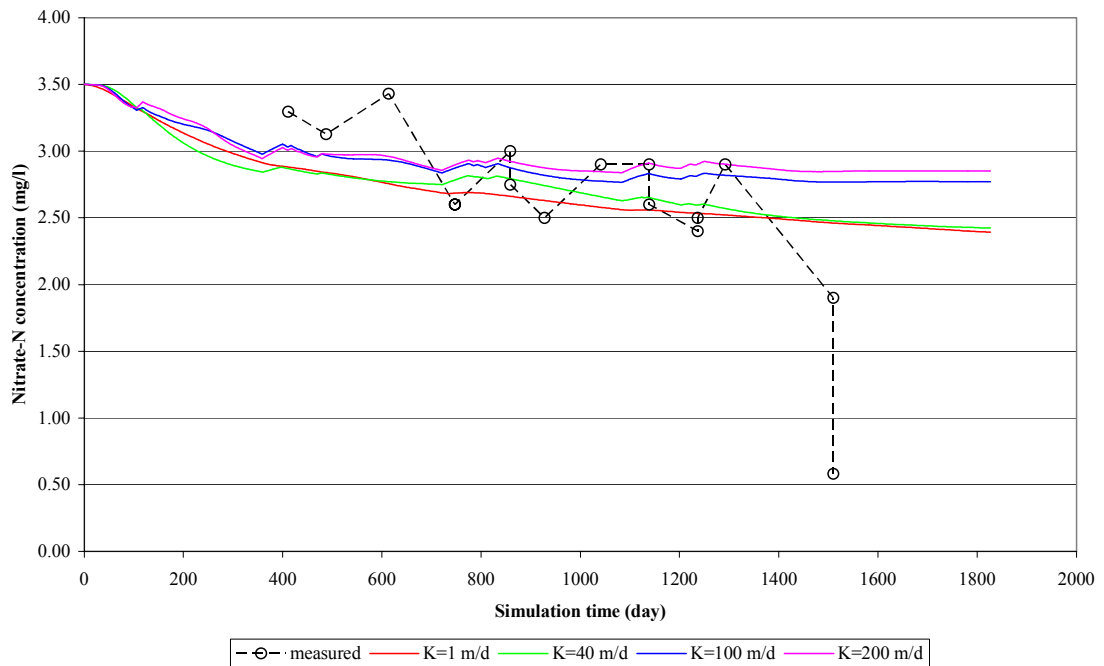


Figure 27: Comparison between measured and simulated BTCs at monitoring well 5

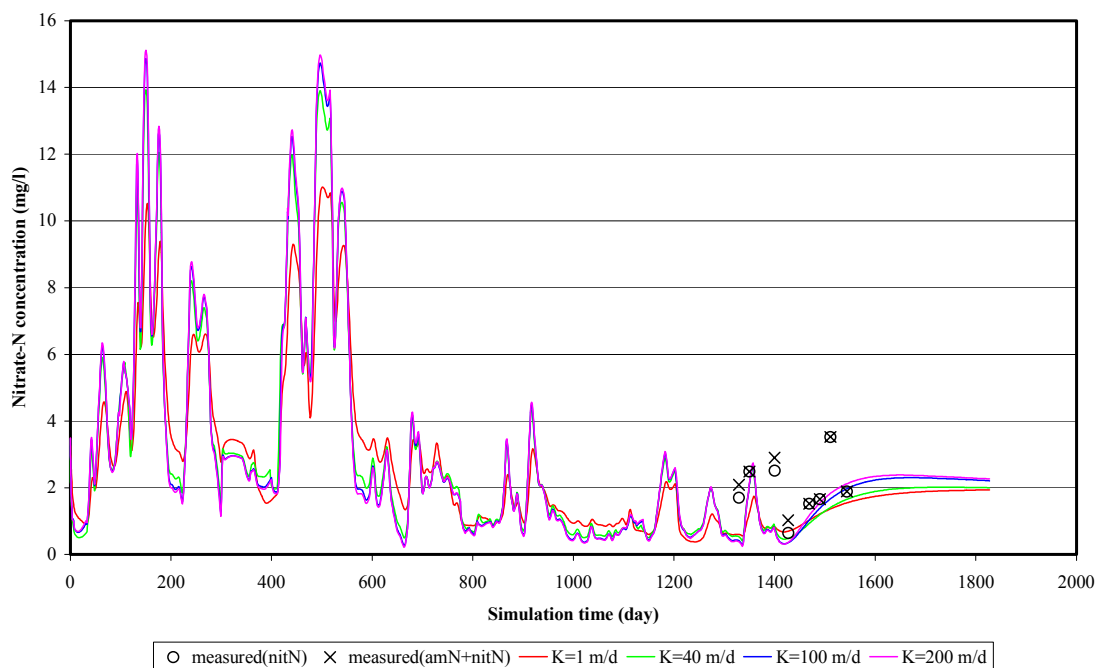


Figure 28: Comparison between measured and simulated BTCs at monitoring well 6

Figure 28 and Figure 29 show that when the hydraulic conductivity is increased, even by a factor of 200, no shift in the peaks of nitrate plume is discernable at wells 6 and 7. This demonstrates that the groundwater flow velocity at the immediate downstream of the discharge trench is dominated by the effluent discharge rate. The reason for this is that wells 6 and 7 are very close to the discharge trench and the average effluent discharge velocity, about 0.6 m/day, is larger than the regional

groundwater flow velocity, which is only 0.002 m/day for the case of $K=1$ m/day and 0.4 m/day for the case of $K=200$ m/day. With the increase in the distance away from the trench, the effect of mixing between effluent and background water becomes apparent and thus the effect of regional flow velocity on peak arrival times is observable as is shown in Figure 30 to Figure 32.

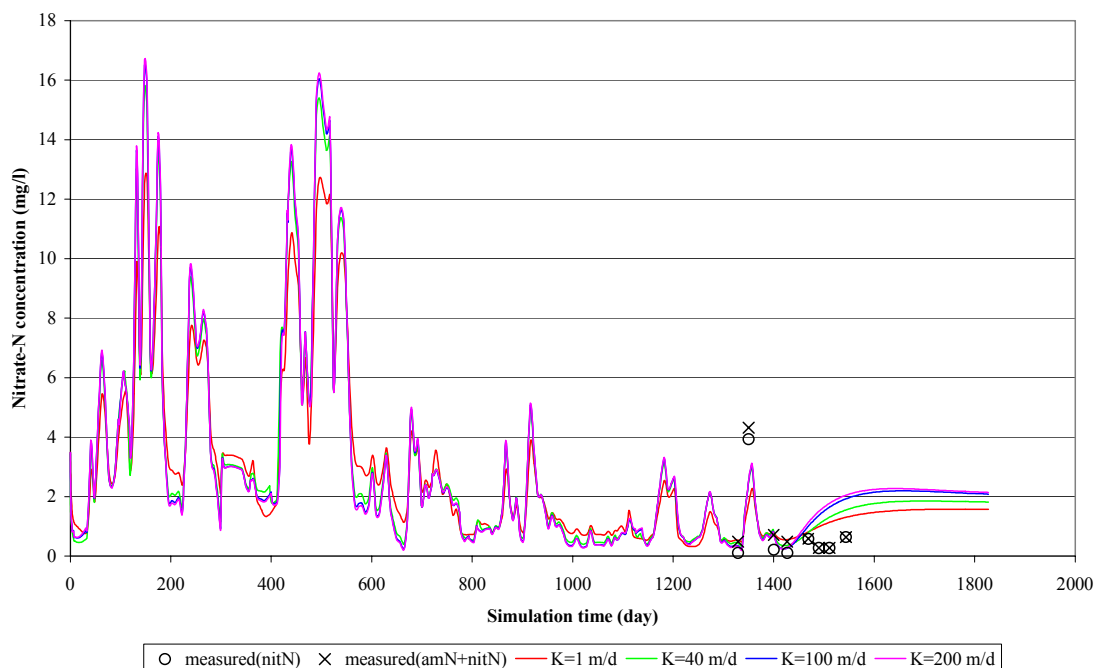


Figure 29: Comparison between measured and simulated BTCs at monitoring well 7 for various values of hydraulic conductivity

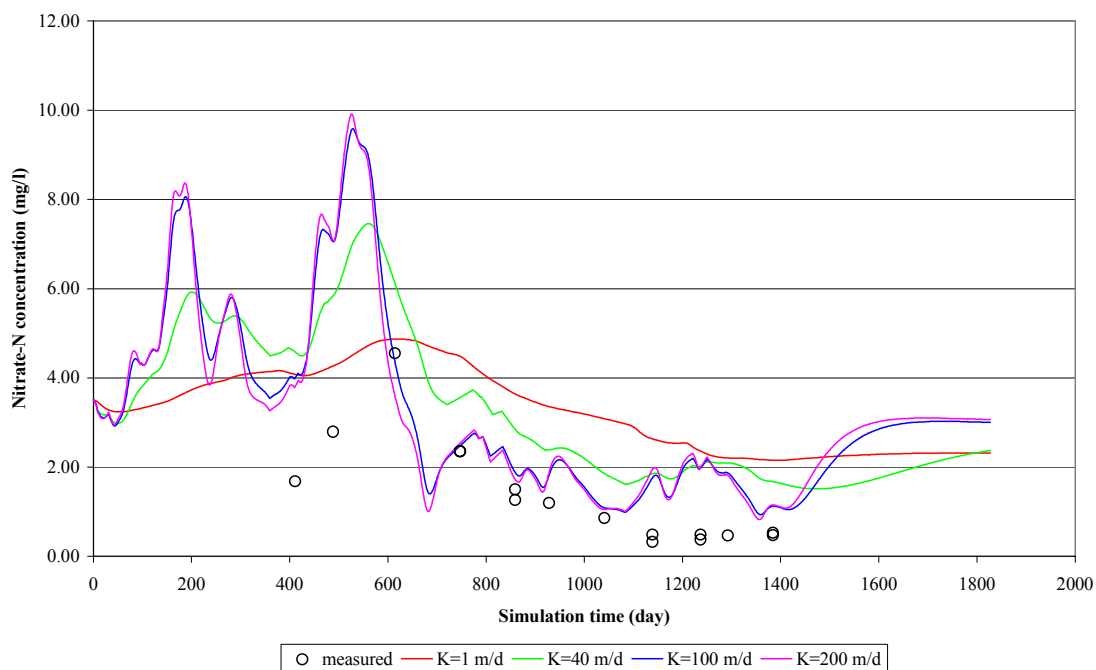


Figure 30: Comparison between measured and simulated BTCs at monitoring well 2 for various values of hydraulic conductivity

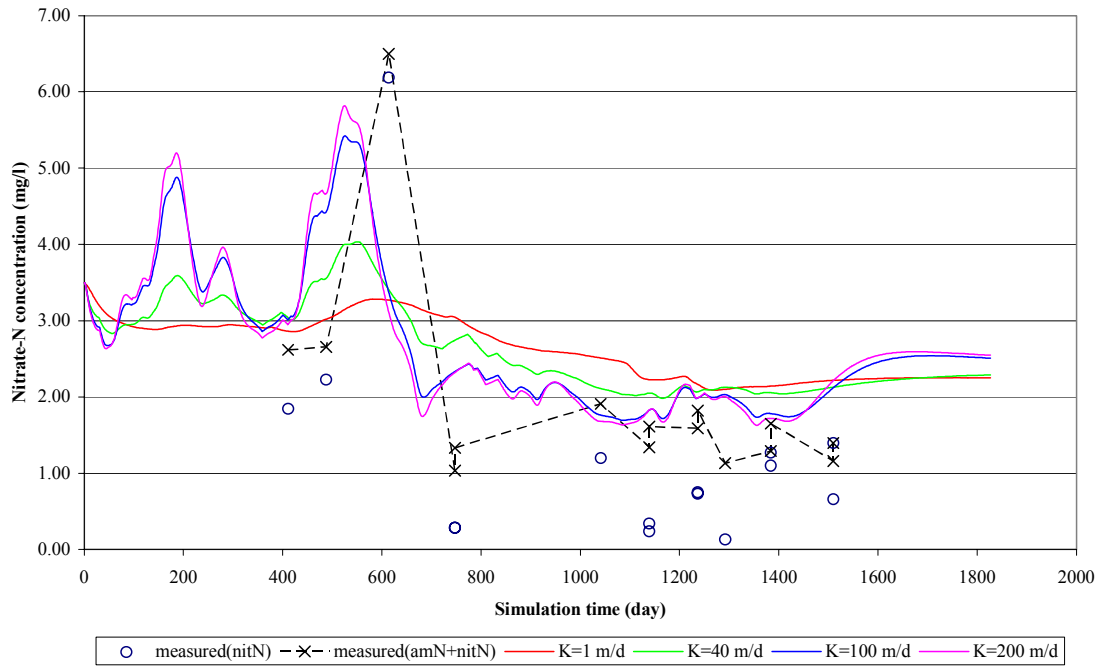


Figure 31: Comparison between measured and simulated BTC's at monitoring well 3 for various values of hydraulic conductivity

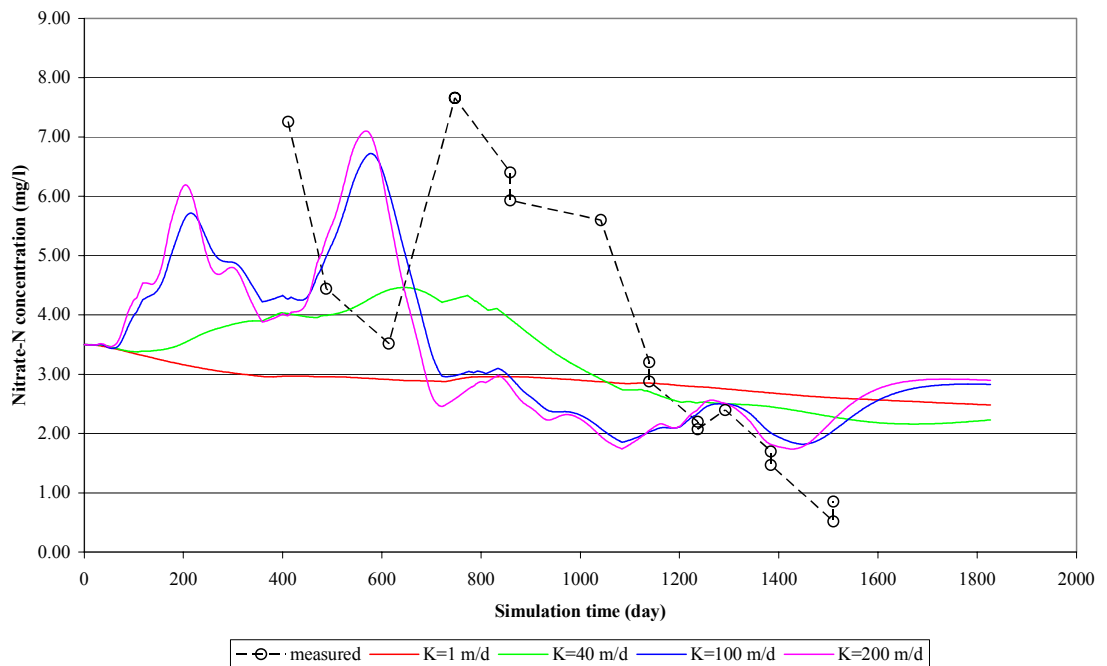


Figure 32: Comparison between measured and simulated BTC's at monitoring well 4 for various values of hydraulic conductivity

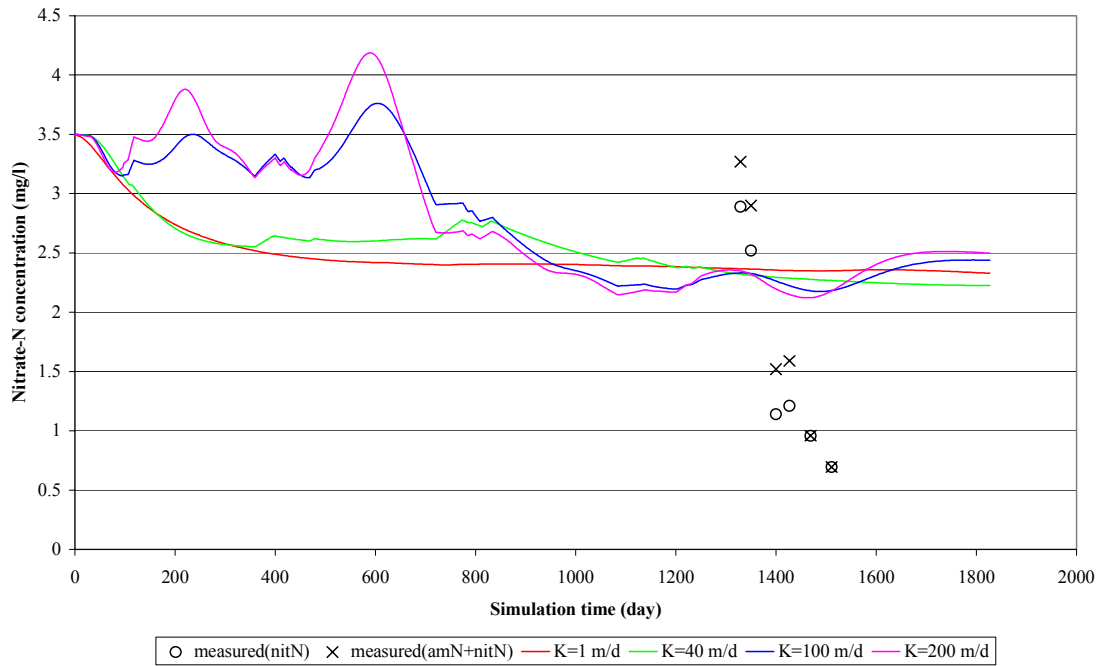


Figure 33: Comparison between measured and simulated BTCs at monitoring well 8 for various values of hydraulic conductivity

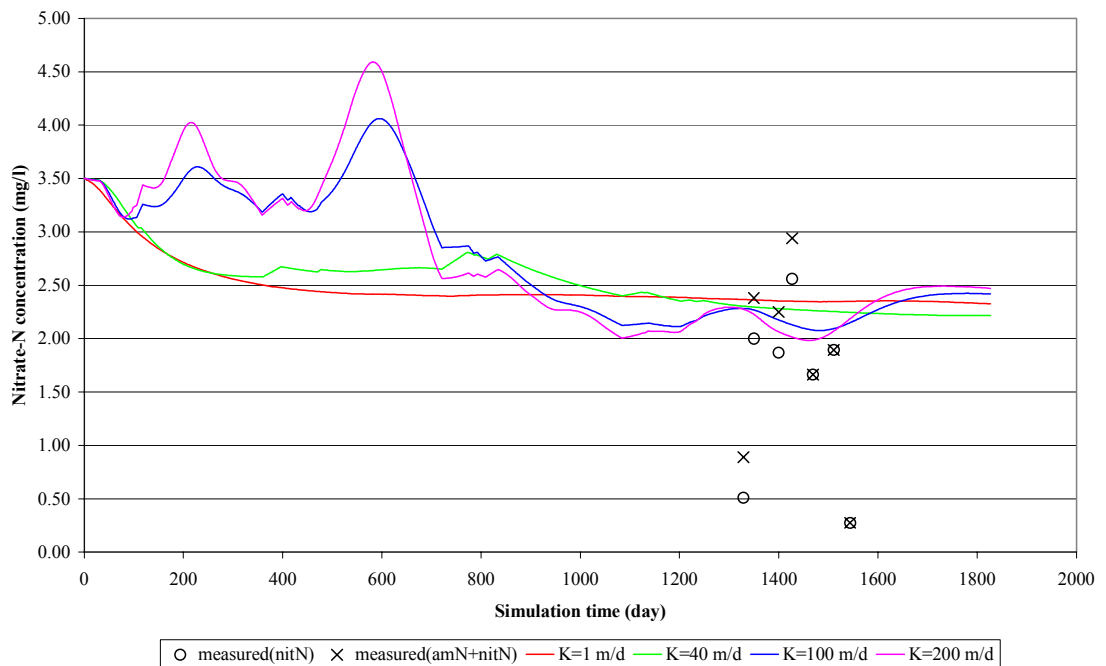


Figure 34: Comparison between measured and simulated BTCs at monitoring well 9 for various values of hydraulic conductivity

12 KINLOCH SBR MODEL SENSITIVITY ANALYSIS

The sensitivity of the simulated BTCs at the monitoring wells to model parameters, which were not measured, is discussed below.

12.1 Hydraulic Conductivity

As discussed in Section 9, monitoring wells 1 (control) and 5 (Figure 26 and Figure 27) are outside of the SBR plume. The simulation reduction in nitrate-N concentrations in these two wells is due to the dilution of the shallow groundwater from the rainfall-recharge water into the shallow water table. The lower hydraulic conductivity rates (1 m and 40 m/day) were not able to provide the more dynamic measured response observed in well 4, which is further away from the SBR trench than the closer wells 2 and 3. The period of monitoring in wells 8 and 9 is relatively short compared to the other monitoring wells and difficult to interpret in terms of matching simulated to measured values. The nitrate-N concentrations in these two wells is also as low as the well 1 (control) and well 5 which are outside of the SBR plume. The two closest wells (wells 6 and 7) show very little difference in the simulated nitrate-N values with differing hydraulic conductivities due to the short distance of travel in the groundwater as discussed in Section 6.1. The model was better able to describe the nitrate-N concentrations in well 6, when the discharge through the trench was no longer being used, than in well 7. Well 6 showed an increase in the nitrate-N concentrations during this period which was also simulated, but was not observed in well 7. The fit is also better in the close wells (wells 3, 6 and 7) when compared to the total amount of inorganic nitrogen present, rather than just nitrate-N. This is probably due to dissimilarity nitrate-N reduction within the plume close to the SBR discharge trench, as discussed by Barkle (2004). The 150 m/day hydraulic conductivity value gave the best fit to the measured data in wells 2 to 4 (Figure 30 to Figure 32) where the influence on the nitrate-N concentrations due to the hydraulic conductivity could be more easily differentiated.

With the higher hydraulic conductivities ($K > 40$ m/day), the effluent discharge rates of approximately 0.6 m/day did not cause the occurrence of groundwater mounding. In the case when K was only 1 m/day, groundwater mounding occurs when the effluent discharge rate was larger than 1m/day.

12.2 Rate of Denitrification

The effect of denitrification on nitrate-N concentrations on monitoring wells 2 to 4 and 6 to 9 is shown in Figure 35 to Figure 41. The calibrated hydraulic conductivity of 150 m/day is used in these simulations. In the wells where the nitrate-N concentration is low (wells 8 and 9; Figure 40 and Figure 41, respectively), the effect of increasing the denitrification rate from 0.1 to 2.0 mg/l/day is not discernable. In the close wells (wells 2 to 4), the higher rate of denitrification was able to better predict the nitrate-N concentration, especially in well 2. As discussed previously, the fit is better when the total amount of inorganic N is considered rather than just the nitrate-N concentrations in these closer wells. The denitrification rate of 1.0 mg/l/d gave the best fit to all of the measured data.

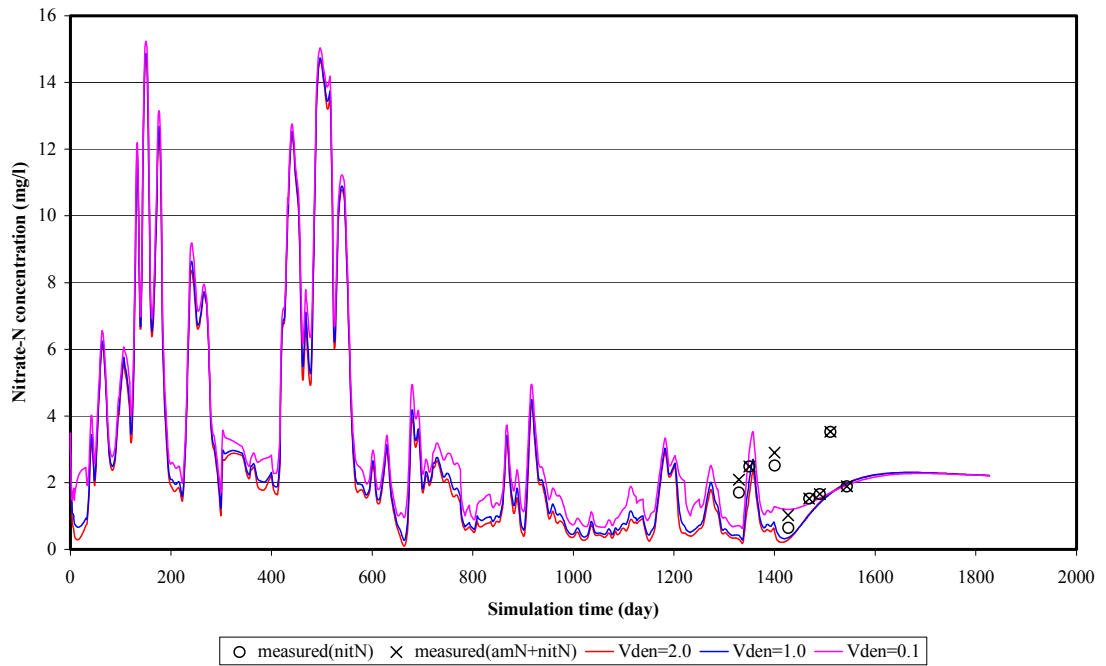


Figure 35: Simulated BTC at monitoring well 6 as affected by the rate of denitrification (V_{den})

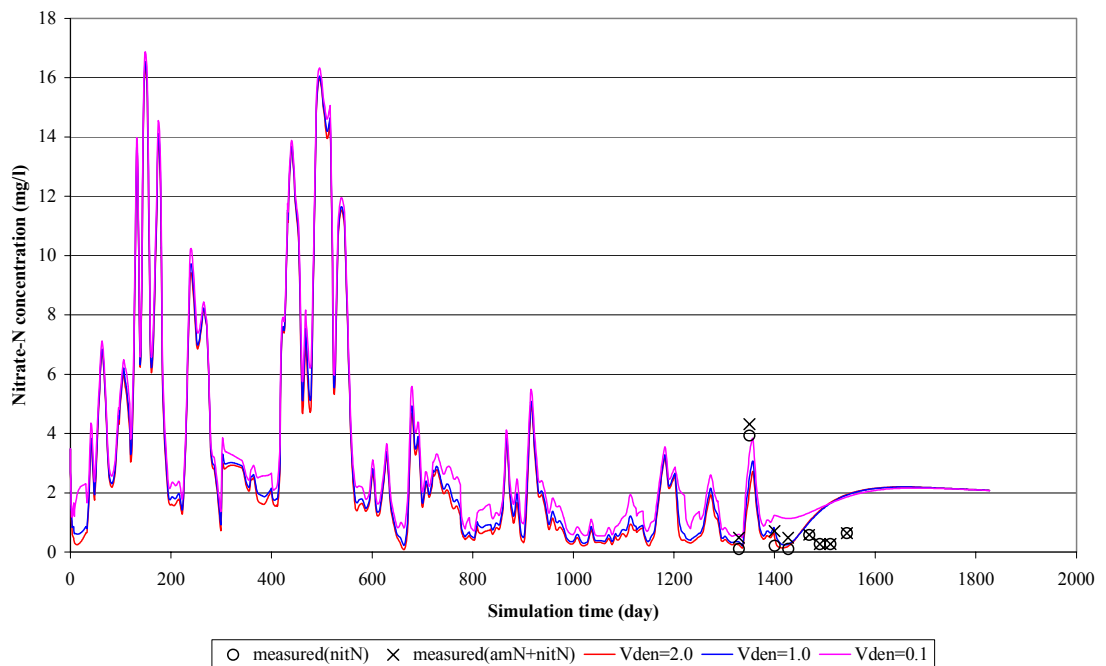


Figure 36: Simulated BTC at monitoring well 7 as affected by the rate of denitrification (V_{den})

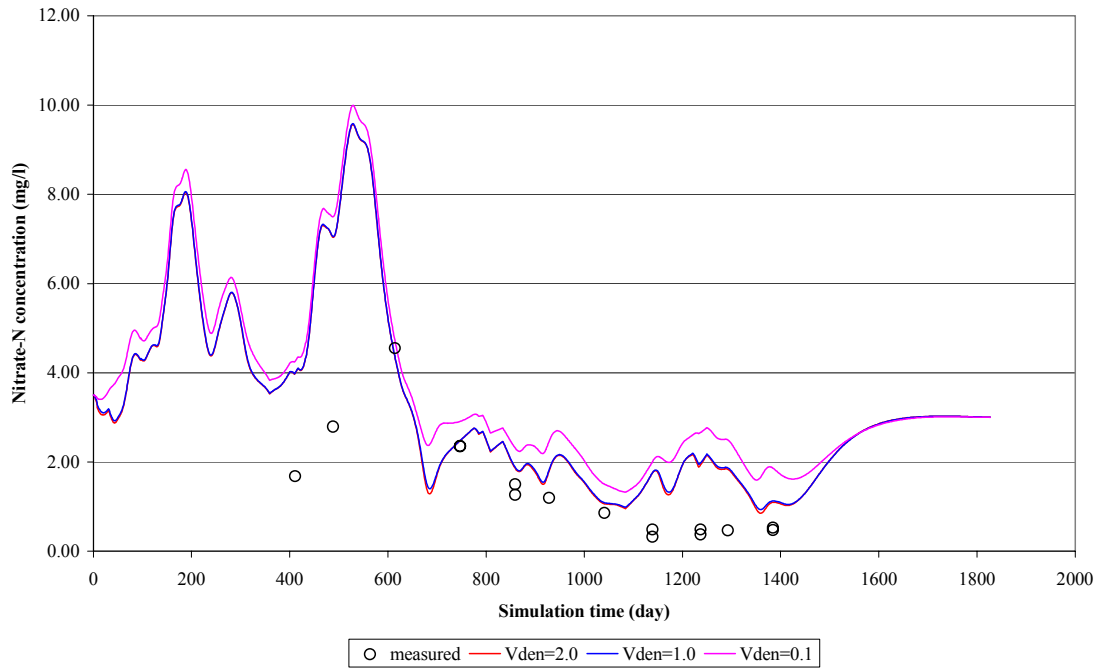


Figure 37: Simulated BTC at monitoring well 2 as affected by the rate of denitrification (V_{den})

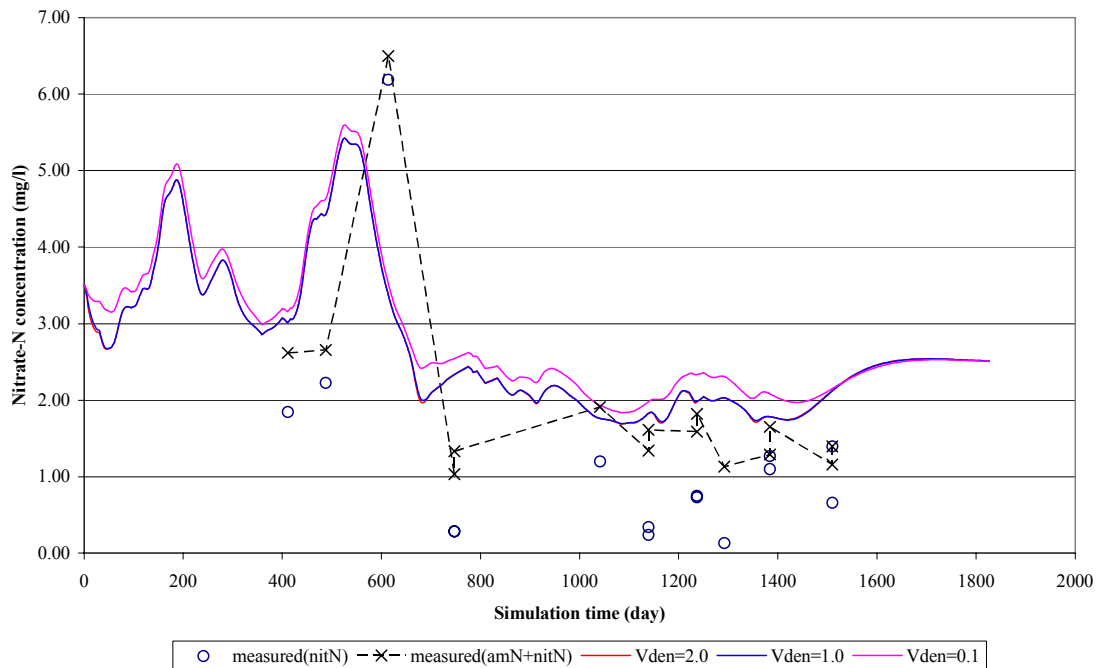


Figure 38: Simulated BTC at monitoring well 3 as affected by the rate of denitrification (V_{den})

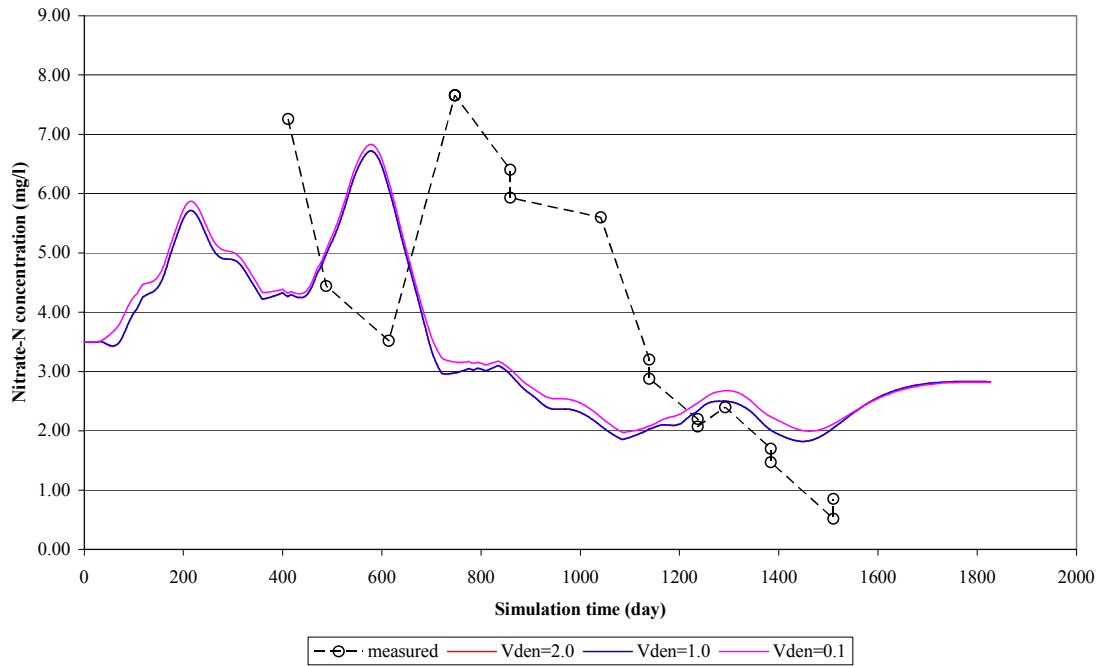


Figure 39: Simulated BTC at monitoring well 4 as affected by the rate of denitrification (V_{den})

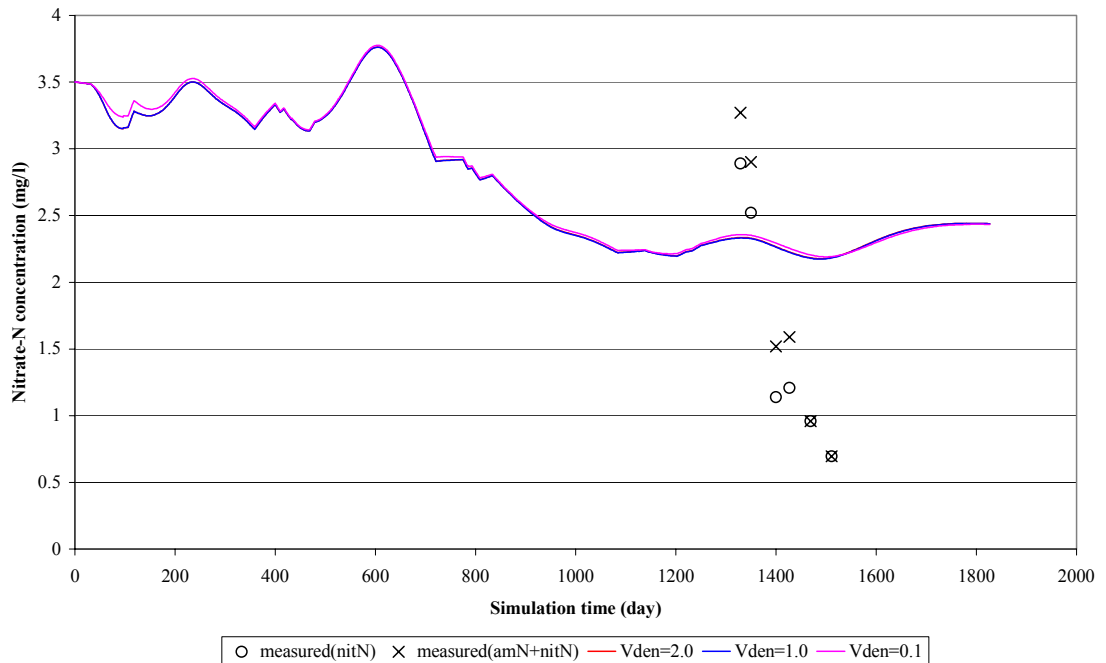


Figure 40: Simulated BTC at monitoring well 8 as affected by the rate of denitrification (V_{den})

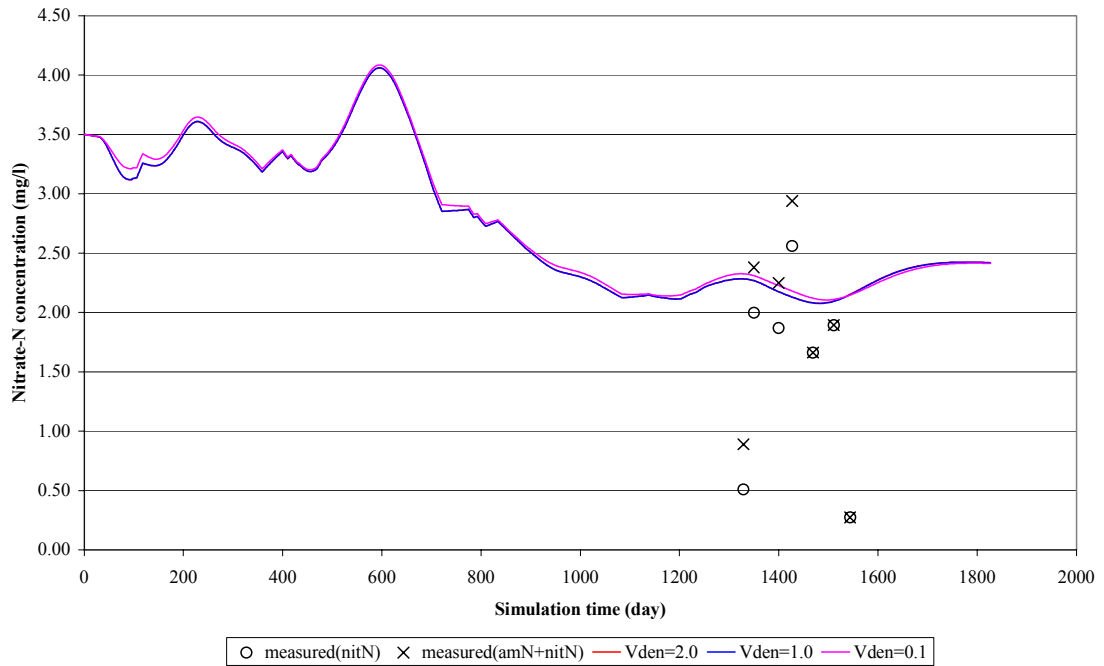


Figure 41: Simulated BTC at monitoring well 9 as affected by the rate of denitrification (*Vden*)

12.3 Rate of Nitrification

The effect of the rate of nitrification on nitrate-N concentrations at monitoring wells 2 to 4 and 6 to 9 is shown in Figure 42 to Figure 48. In wells 8 and 9, where the ammonium concentrations are at the lowest, the effect of the nitrification rate on the nitrate-N concentration is also at its lowest. The best fit, which can be seen in Figure 42 to Figure 46, is from the nitrification rate of 0.01/day.

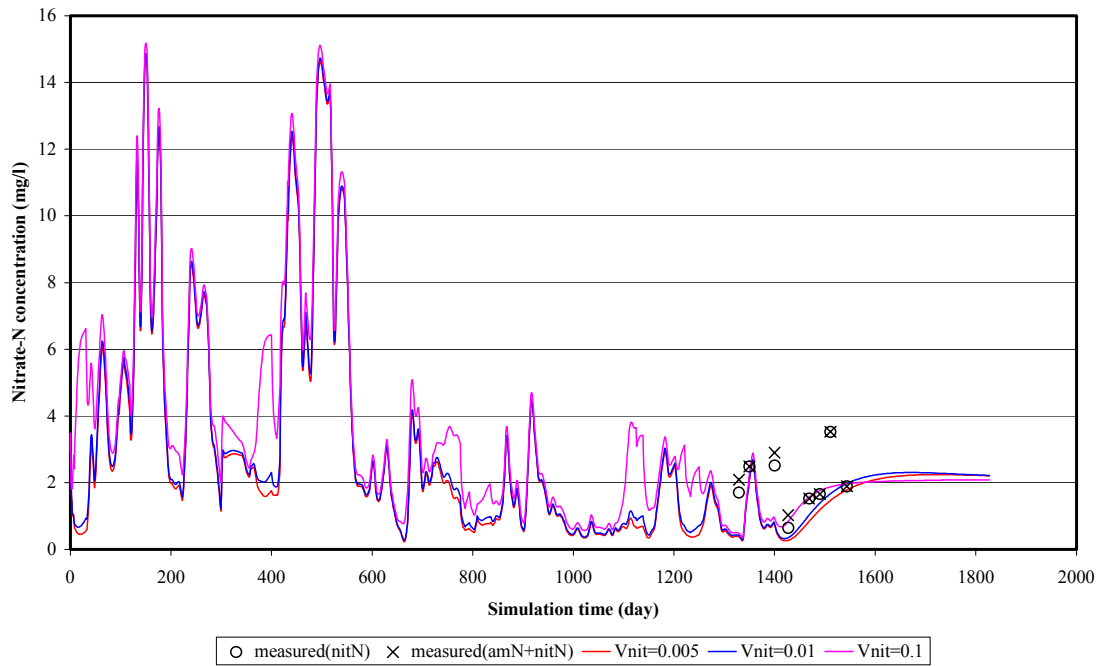


Figure 42: Simulated BTC at monitoring well 6 as affected by the rate of nitrification (V_{nit})

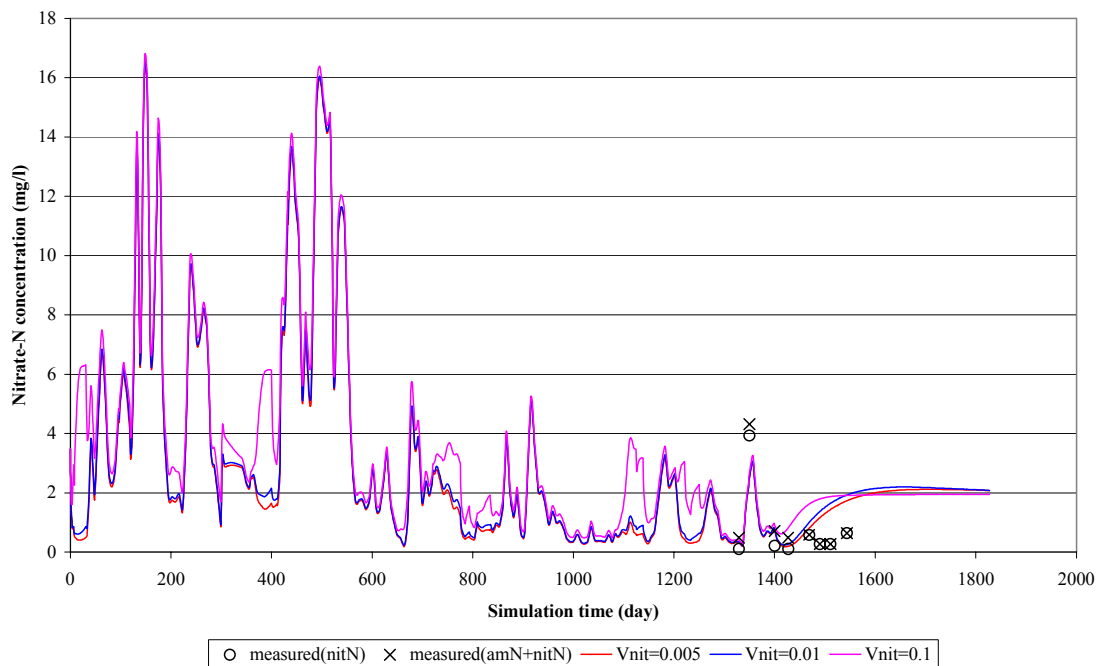


Figure 43: Simulated BTC at monitoring well 7 as affected by the rate of nitrification (V_{nit})

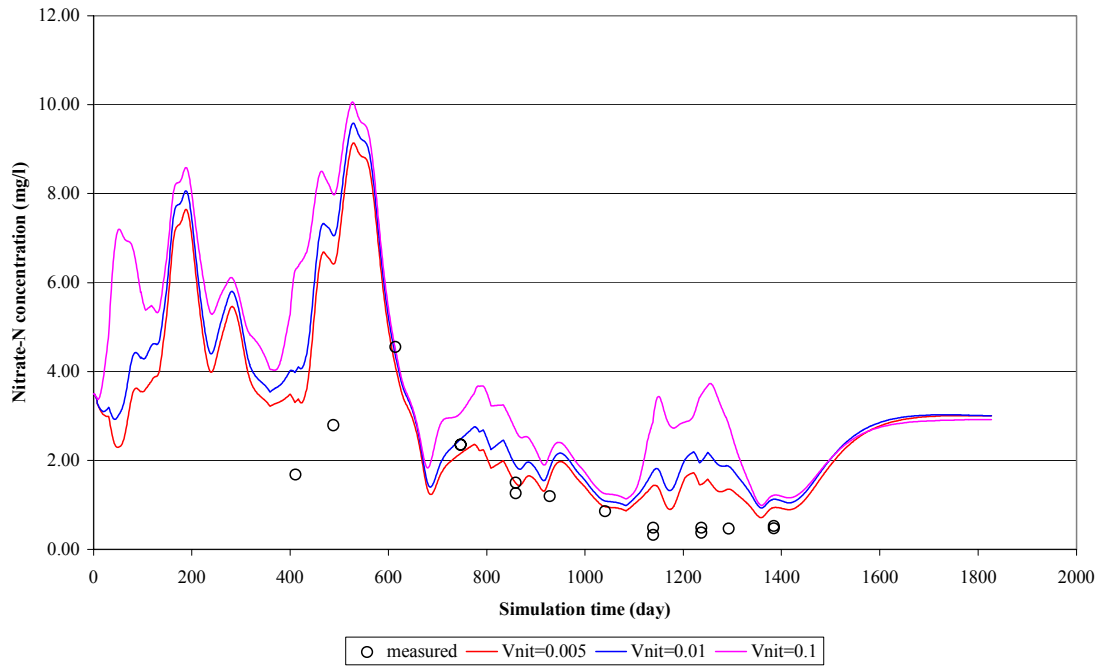


Figure 44: Simulated BTC at monitoring well 2 as affected by the rate of nitrification (Vnit)

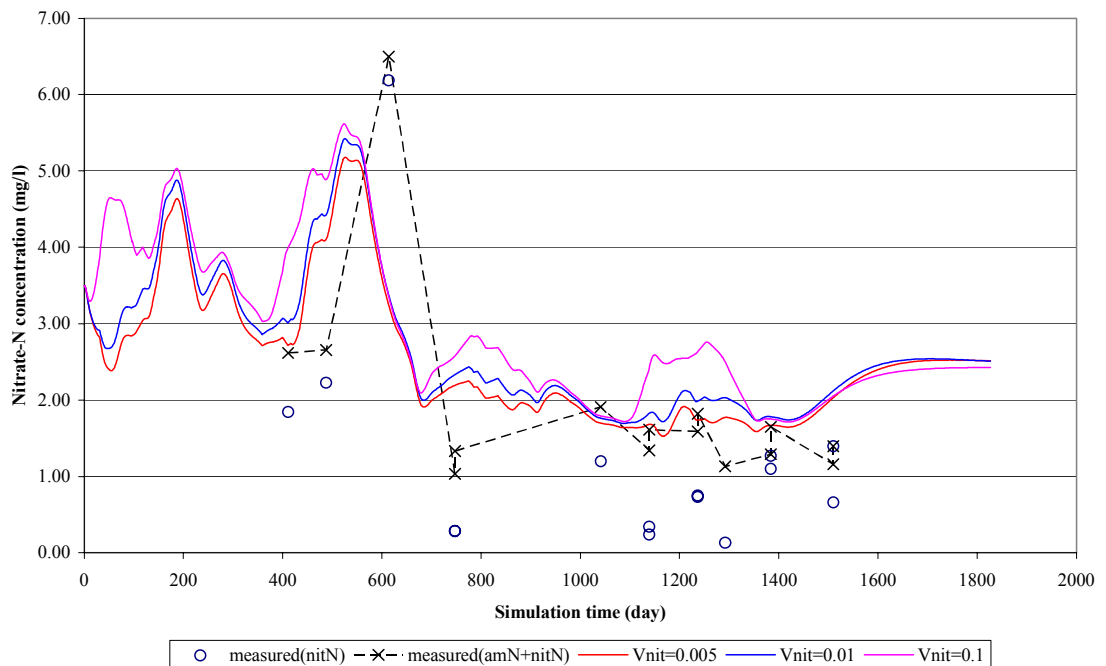


Figure 45: Simulated BTC at monitoring well 3 as affected by the rate of nitrification (Vnit)

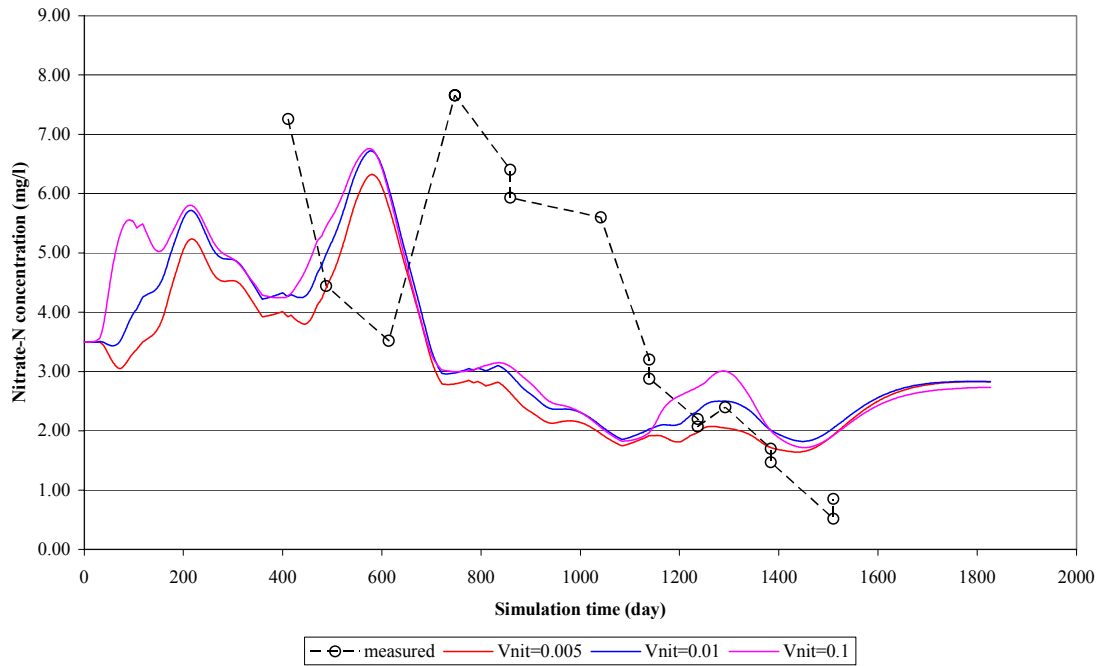


Figure 46: Simulated BTC at monitoring well 4 as affected by the rate of nitrification (V_{nit})

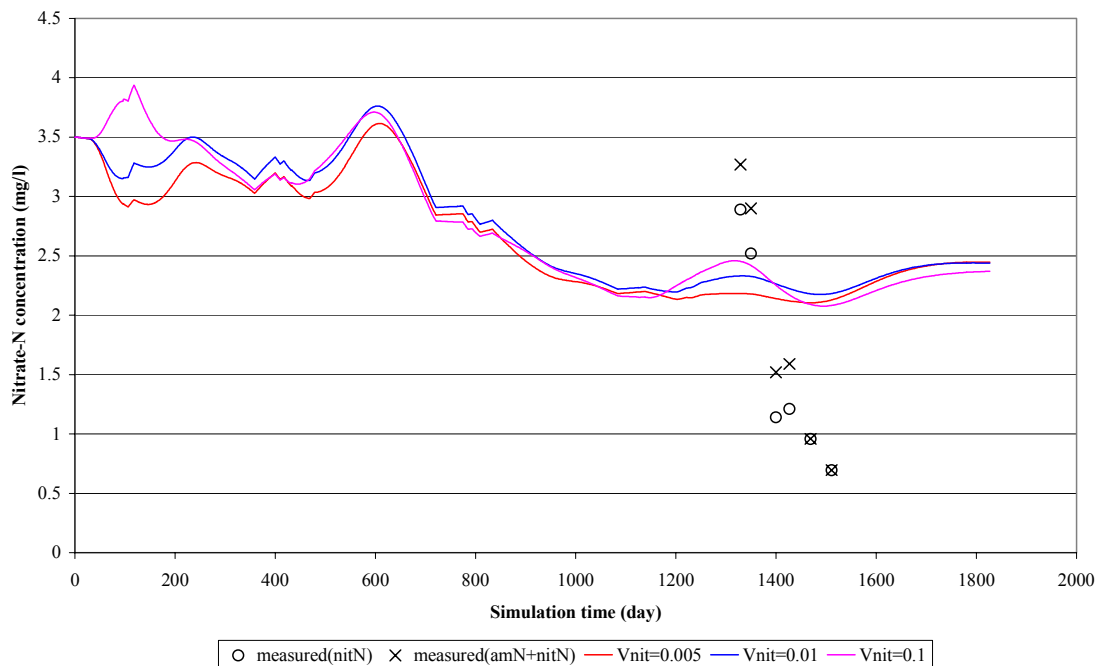


Figure 47: Simulated BTC at monitoring well 8 as affected by the rate of nitrification (V_{nit})

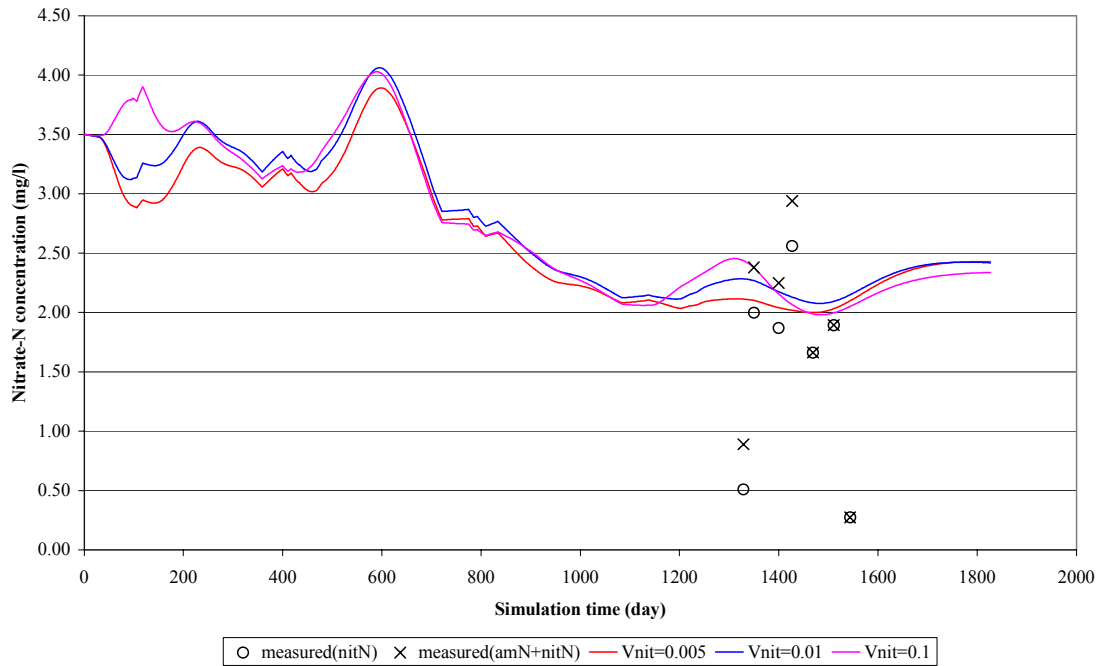


Figure 48: Simulated BTC at monitoring well 9 as affected by the rate of nitrification (V_{nit})

12.4 Dispersion Coefficient

The effect of dispersivity on nitrate-N concentrations at monitoring wells is shown in Figure 49 to Figure 57. The effect of dispersion is more significant in wells further away from the trench than wells close to the trench. The greatest effect of dispersion on nitrate-N concentrations is seen in the upstream well 1 and well 5, which are considered to be outside the SBR plume. The measured nitrate-N concentrations in well 5 oscillates between the two levels of nitrate-N concentration predicted by the dispersion parameters. In this well and well 1 (control), the simulated nitrate-N concentrations are diluted due to rainfall recharge into the shallow aquifer. The greater the distance the wells are from the source of the effluent, the higher the effect of dispersion; however, the lower the nitrate-N concentrations. In wells 8 and 9 (Figure 56 and Figure 57), due to the limited period of data collection and the low absolute values of nitrate-N, it is difficult to determine the effect of dispersion on the nitrate-N concentrations. In Figure 51 to Figure 55 (wells 6 and 7, 2 to 4), the best fit of the simulated nitrate-N concentration to measured data is from longitudinal dispersivity of 5.0 m, horizontal and vertical transpervivities of 1.0 m and 0.1 m, respectively. The ratios of longitudinal to transverse dispersivities are in the range of values given in Zheng and Bennett (1995).

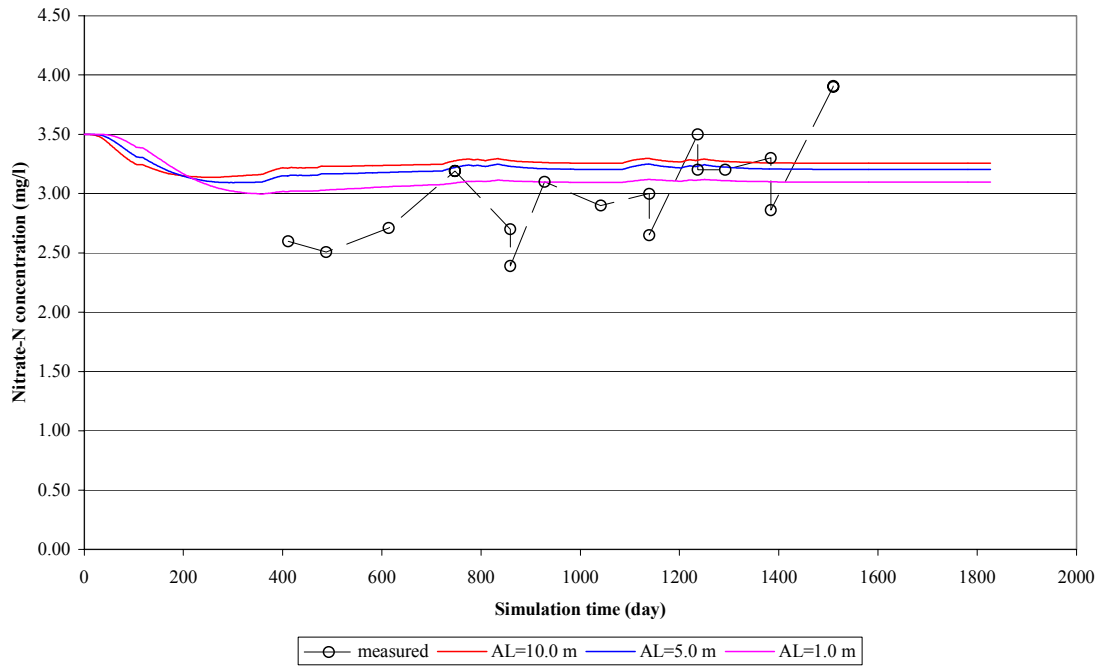


Figure 49: Simulated BTC at monitoring well 1 (control) as affected by longitudinal dispersivity (AL)

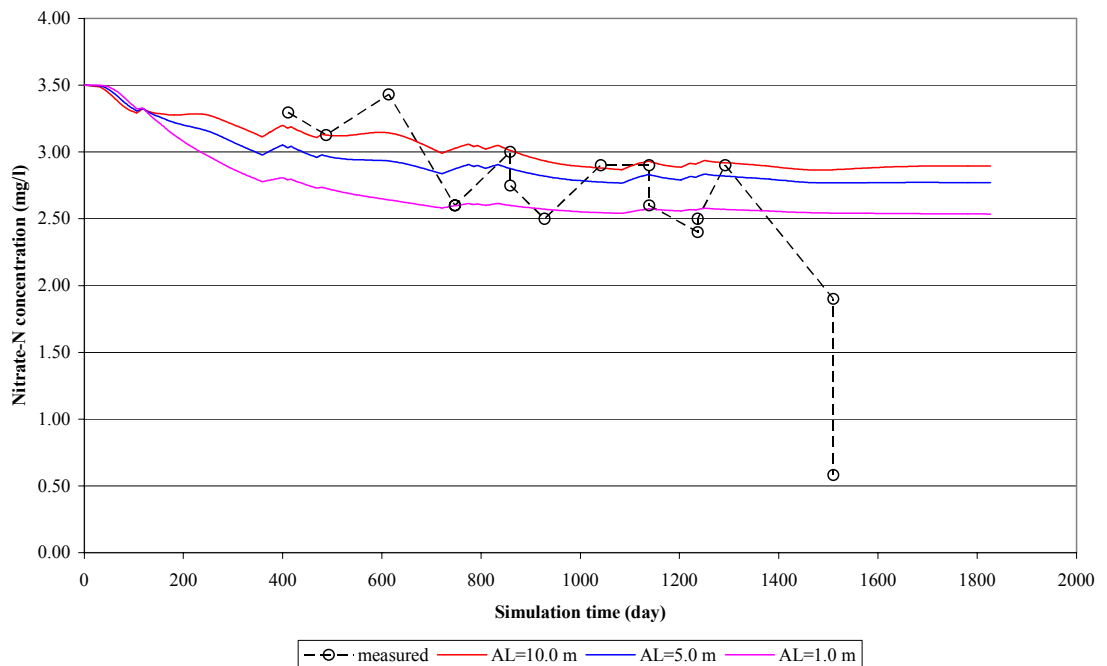


Figure 50: Simulated BTC at monitoring well 5 as affected by longitudinal dispersivity (AL)

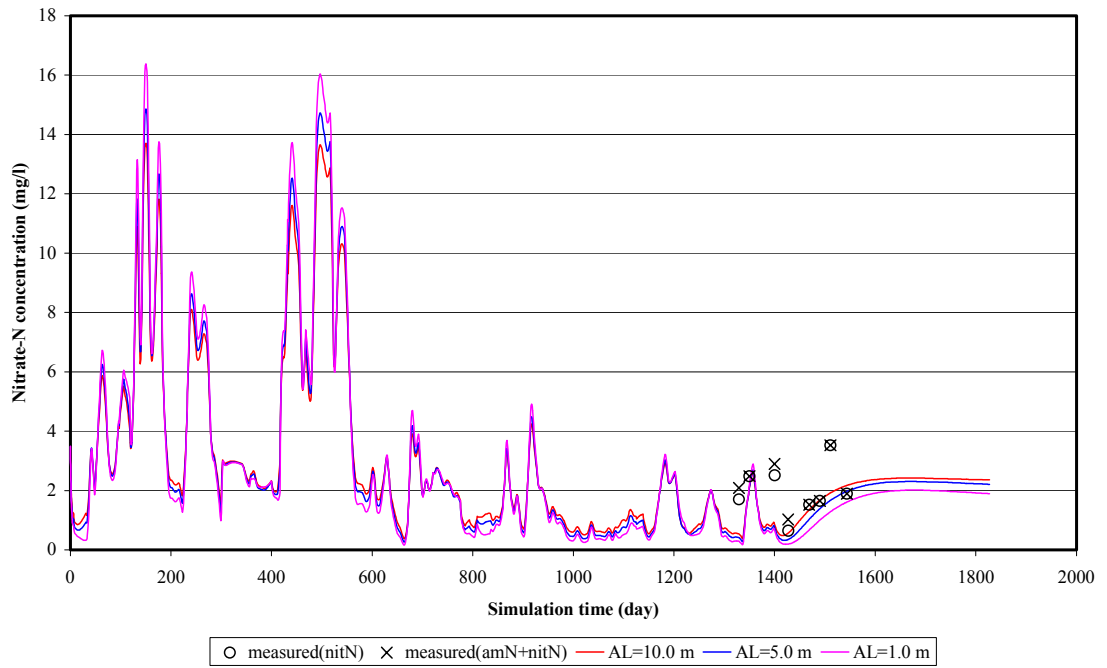


Figure 51: Simulated BTC at monitoring well 6 as affected by longitudinal dispersivity (AL)

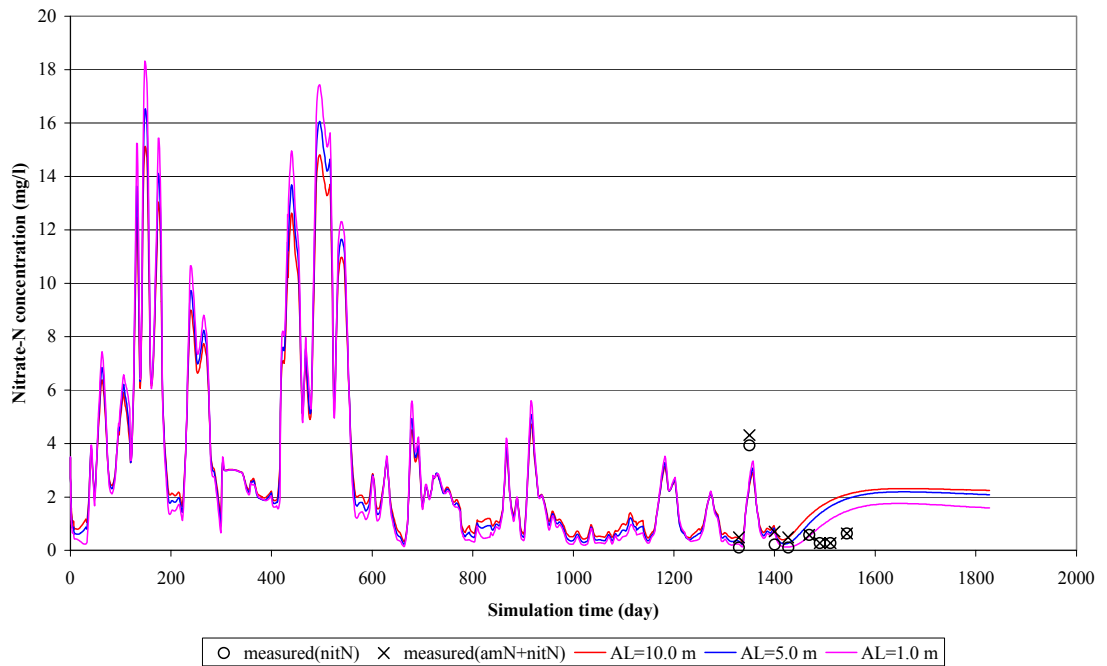


Figure 52: Simulated BTC at monitoring well 7 as affected by longitudinal dispersivity (AL)

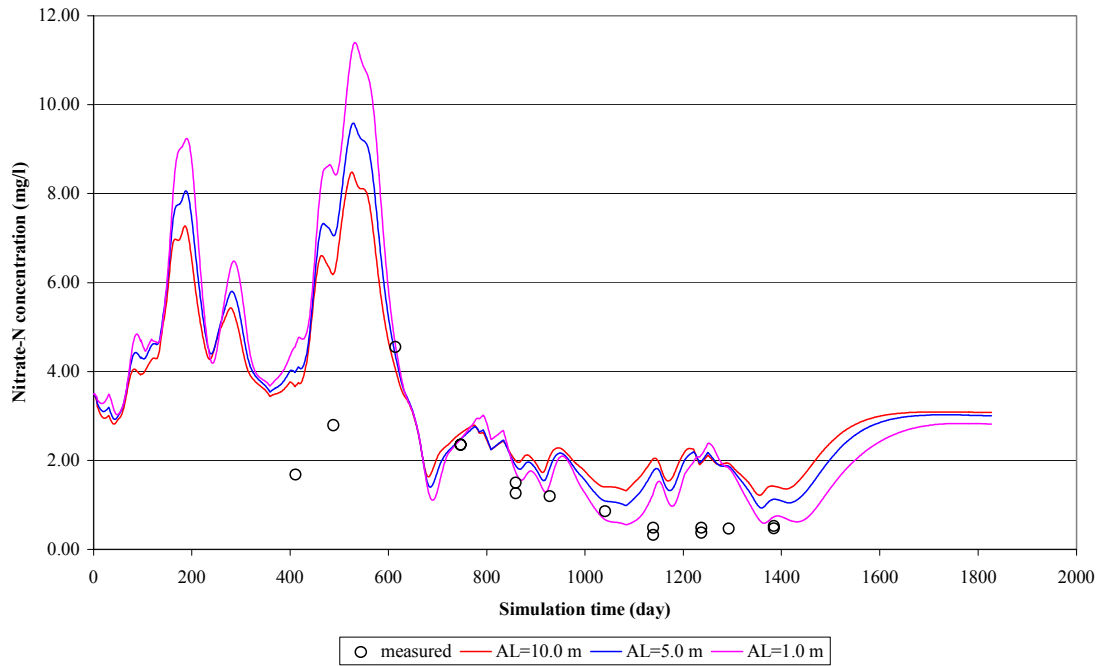


Figure 53: Simulated BTC at monitoring well 2 as affected by longitudinal dispersivity (AL)

In Figure 53, the reason that the lower dispersion value (AL=1.0 m) initially predicts higher nitrate-N concentrations than the higher dispersion value (AL=10.0 m) and then the reverse occurs can be explained as below.

The incoming groundwater from upstream boundary has a concentration of 3.5 mg/l nitrate-N. When the nitrate-N concentration of the discharged effluent is larger than 3.5 mg/l, the concentration will decrease due to the mixing of effluent with the incoming groundwater water. The larger the dispersivity (i.e. better mixing), the smaller the concentration. This results in higher concentrations for the lower dispersivity case (AL=1.0 m).

On the contrary, when the effluent concentration is smaller than 3.5 mg/l nitrate-N, the concentration will be elevated due to the mixing of effluent and the incoming groundwater. Thus the larger the dispersivity, the more the concentration is elevated. This results in higher concentrations for the larger dispersivity case (AL=10.0 m).

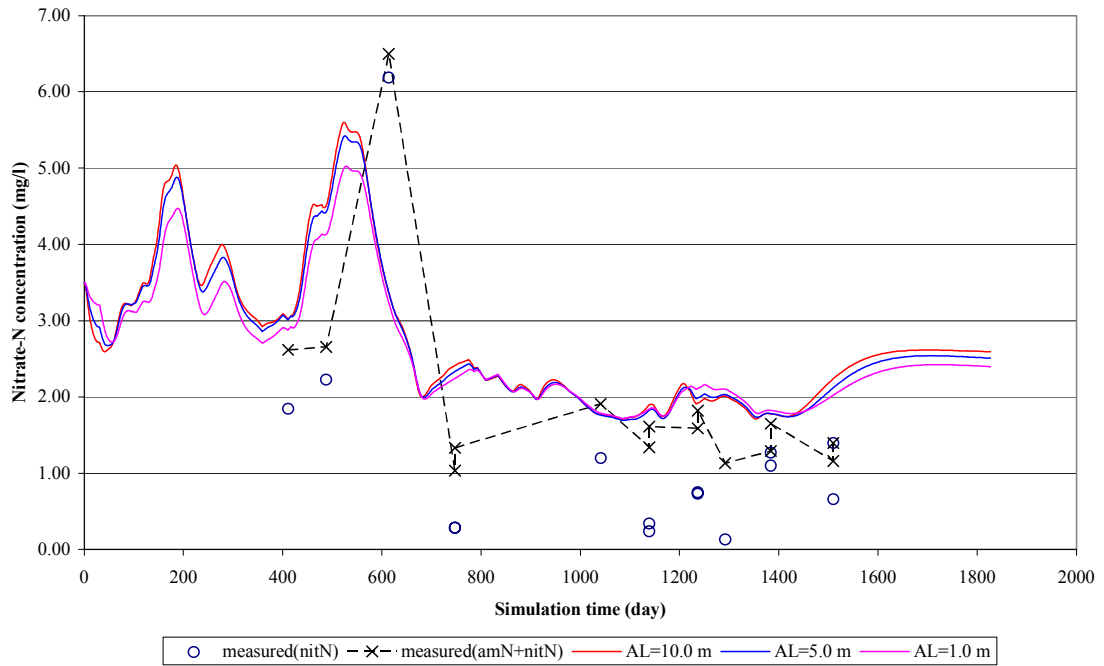


Figure 54: Simulated BTC at monitoring well 3 as affected by longitudinal dispersivity (AL)

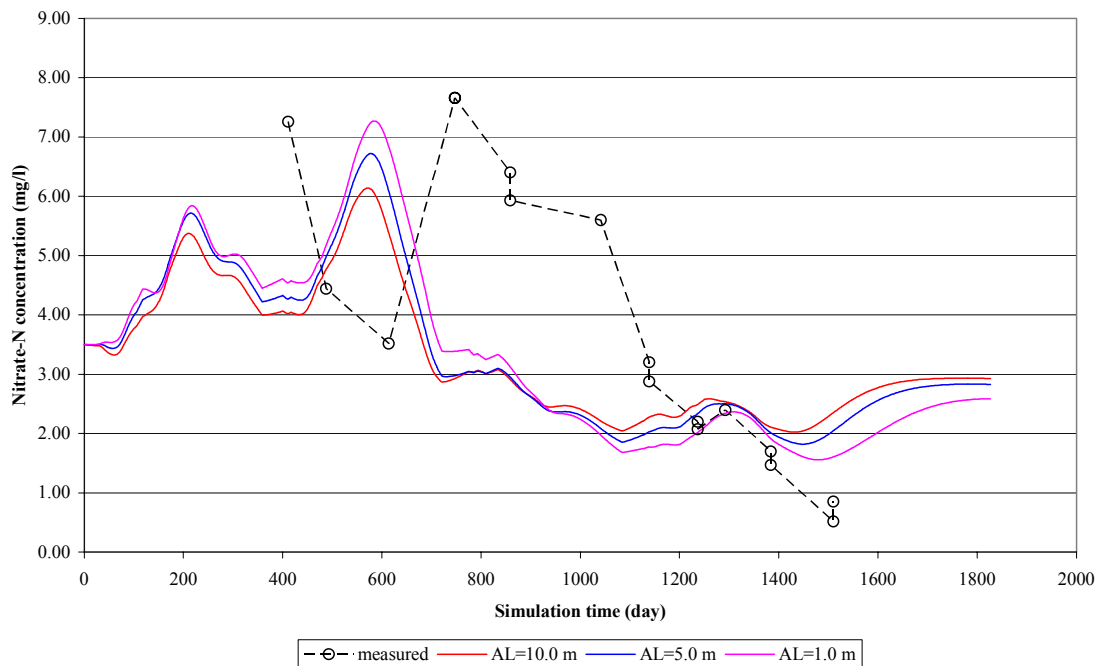


Figure 55: Simulated BTC at monitoring well 4 as affected by longitudinal dispersivity (AL)

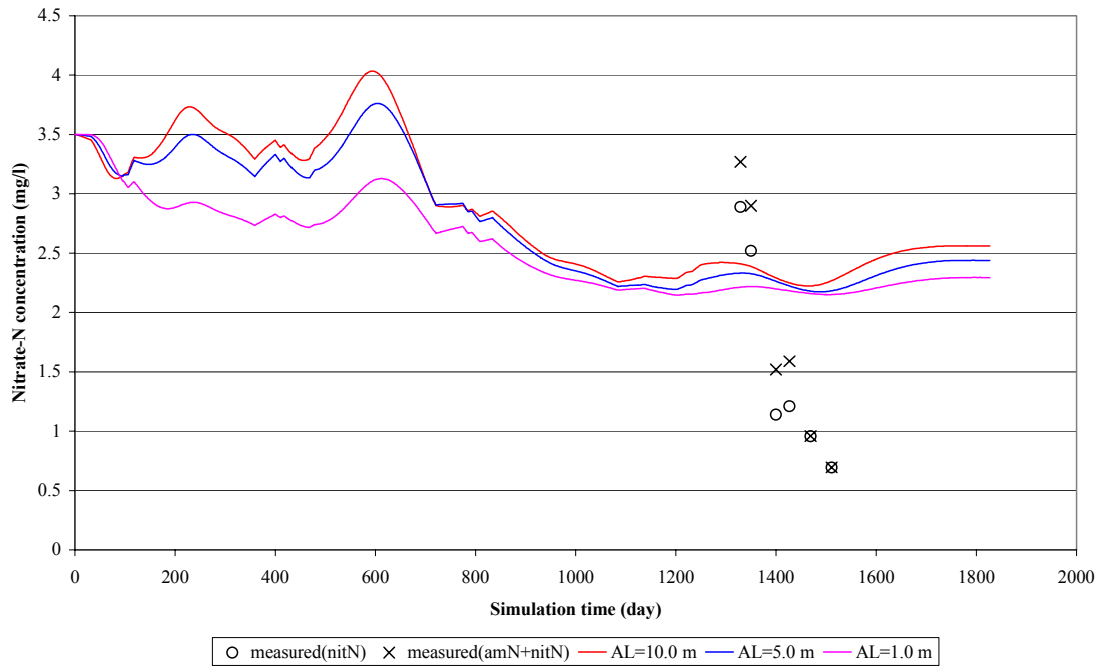


Figure 56: Simulated BTC at monitoring well 8 as affected by longitudinal dispersivity (AL)

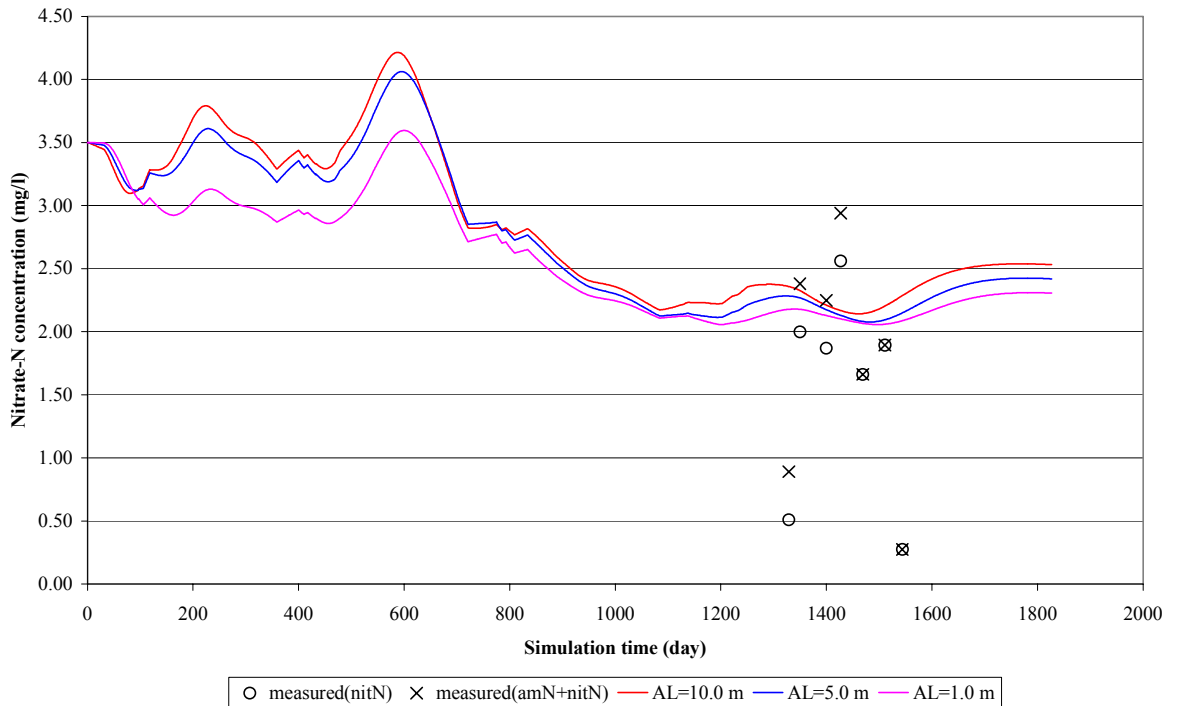


Figure 57: Simulated BTC at monitoring well 9 as affected by longitudinal dispersivity (AL)

13 SUMMARY

The BTCs of nitrate-N concentrations in the monitoring wells from the discharge of treated effluent from the SBR plants at Acacia Bay and Kinloch have been modelled through a 3-D flow and contaminant transport model, FEMWATER-N. Model parameters have been calibrated by comparing the simulated values against the measured nitrate-N data in the monitoring wells.

Analysis showed that the model parameters that are most sensitive to predicting nitrate-N concentrations in the monitoring wells in order are:

- Hydraulic conductivity;
- Denitrification rate;
- Nitrification rate; and
- Dispersivity.

The required effective hydraulic conductivity parameter in the Acacia Bay model agreed well with the measured data. However, the Kinloch model required conductivity that was 150 times greater than that estimated from slug tests. It is possible that the slug test underestimated the aquifer hydraulic conductivity due to the wells not being developed properly. A Monte Carlo analysis showed that the spatial variability of the hydraulic conductivity field within the aquifer could be the major factor for the discrepancy between model predicted concentrations and measured ones.

14 REFERENCES

- Barkle, GF (2004): Acacia Bay and Kinloch SBR groundwater models – Comparison against monitoring data. Report No HA03100/01. Aqualinc Research Ltd.
- Barkle, GF and Wang, F (2003): The simulated fate of treated domestic effluent discharge into the vadose zone within the Taupo catchment. Report No 4949. Lincoln Environmental, a division of Lincoln Ventures Ltd.
- Gomez-Hernandez, JJ and Srivastava, RM (1990): ISIS3D – AnANSI-C three dimensional multiple indicator conditional simulation program. *Computers and Geosciences* **16**:395-440.
- Hadfield, JC (1995): A groundwater contaminant tracer study at Waitahanui, Taupo. Master of Philosophy thesis, Earth Sciences, University of Waikato.
- Hadfield, J and Barkle, GF (2004): Contrasting effects of nitrogen discharge to groundwater from a woolshed and nearby wastewater plant in Taupo catchment. *NZ Hydrology Society Annual Meeting, "The Water Balance", Queenstown, November 2004.*
- Hadfield, JC and Piper, J (2005): Unpublished slug test data. Environment Waikato. Personal communications.
- Kinloch, (1998): A history of Kinloch – published in conjunction with the Kinloch silver Jubilee 1959-1984.
- Wang, F; Bright, J; Hadfield, J (2003): Simulating nitrate-N transport in an alluvial aquifer – A three-dimensional N-dynamics model. *Journal of Hydrology (NZ)* **42(2)**:145-162.
- Zheng, C and Bennett, GD (1995): *Applied contaminant transport modelling – Theory and practice*. Van Nostrand Reinhold, New York, pp245-249.